

WA
630.7
661
62
1978 c.3

WASHINGTON STATE LIBRARY
STATE OF WASHINGTON
OLYMPIA, WASHINGTON

DEPARTMENT OF NATURAL RESOURCES

BERT L. COLE, Commissioner of Public Lands
RALPH A. BESWICK Supervisor

DIVISION OF GEOLOGY AND EARTH RESOURCES

VAUGHN E. LIVINGSTON, JR., State Geologist

INFORMATION CIRCULAR 62

HEAT FLOW STUDIES
IN THE
STEAMBOAT MOUNTAIN-LEMEI ROCK AREA,
SKAMANIA COUNTY, WASHINGTON

BY

J. ERIC SCHUSTER,
DAVID D. BLACKWELL,
PAUL E. HAMMOND,
and
MARSHALL T. HUNTING

Final report to the
NATIONAL SCIENCE FOUNDATION
on sponsored project
AER75-02747



1978

TION CIRCULAR 62

STATE OF WASHINGTON
DEPARTMENT OF NATURAL RESOURCES

BERT L. COLE, Commissioner of Public Lands
RALPH A. BESWICK Supervisor

DIVISION OF GEOLOGY AND EARTH RESOURCES

VAUGHN E. LIVINGSTON, JR., State Geologist

INFORMATION CIRCULAR

WA
333.7
M66i
62
1978

Heat flow
studies in the
Steamboat
Mountain-Lemei
Rock area,
Skamania County,
Washington

HEAT FLOW STUDIES
IN THE
STEAMBOAT MOUNTAIN-LEMEI ROCK AREA,
SKAMANIA COUNTY, WASHINGTON

BY

**J. ERIC SCHUSTER,
DAVID D. BLACKWELL,
PAUL E. HAMMOND,
and
MARSHALL T. HUNTTING**

Final report to the
NATIONAL SCIENCE FOUNDATION
on sponsored project
AER75-02747



1978

CONTENTS

	<u>Page</u>
Abstract	1
Introduction	2
Acknowledgments	3
Geology	4
General features	4
Cenozoic rocks	10
Quaternary basalts	11
Geophysics	16
Geochemistry	19
Drill holes	23
Site selection	23
Temperatures	23
Bottom-hole temperature measurements	25
Temperature gradients	27
Drill hole DGER 2	27
Drill hole DGER 3	27
Drill hole DGER 4	27
Drill hole DGER 5	30
Drill hole DGER 6	30
Drill hole DGER 7	33
Thermal conductivity determinations	33
Heat flow	35
Discussion	40
Conclusions	43
Appendix—Equilibrium temperature-depth measurements	45
References cited	53

ILLUSTRATIONS

		<u>Page</u>
Figure	1. Generalized geologic map and cross sections of part of the southern Cascade Range, Washington	6
	2. Geologic map of the Indian Heaven area, southern Cascade Range, Washington	8
	3. View to the north from Red Mountain	12
	4. Sawtooth Mountain, looking toward the northeast	14
	5. Broken and jumbled basalt blocks at the edge of the Big Lava Bed in the southern part of the study area	15
	6. Bouguer gravity map of part of the southern Cascade Range, Washington	17
	7. An aeromagnetic map of part of the southern Cascade Range, Washington.....	18
	8. Locations of chemically analyzed springs and rivers in the Cascade Range, Washington	22
	9. Temperature-depth curves for drill holes DGER 2 through 7	24
	10. Temperature-depth curve for drill hole DGER 2	28
	11. Temperature-depth curve for drill hole DGER 3	29
	12. Temperature-depth curve for drill hole DGER 4	31
	13. Temperature-depth curve for drill hole DGER 5	32
	14. Heat-flow map for the Indian Heaven area, Skamania County, Washington	39

TABLES

		<u>Page</u>
Table	1. Cenozoic geologic units of the southern Cascade Range, Washington	5
	2. Quaternary basalts and interbedded cinders and ash in a portion of the southern Cascade Range, Washington	13
	3. Chemical data for springs and rivers in the Cascade Range, Washington	20
	4. Average temperature gradient, thermal conductivity, and heat flow measurements for drill holes DGER 2 through 7	25
	5. Thermal conductivity, density, and porosity measurements for drill holes DGER 2 through 5	26
	6. Lithology of heat-flow drill holes, Steamboat Mountain-Lemei Rock area, Skamania County, Washington	36

HEAT FLOW STUDIES IN THE STEAMBOAT MOUNTAIN-LEMEI ROCK AREA, SKAMANIA COUNTY, WASHINGTON

by
J. Eric Schuster^{1/}
David D. Blackwell,^{2/}
Paul E. Hammond,^{3/}
and
Marshall T. Huntting^{4/}

ABSTRACT

In order to investigate the possible occurrence of geothermal energy in areas of Quaternary basaltic volcanism, the Washington State Department of Natural Resources drilled several 152 m deep heat-flow holes in the Steamboat Mountain-Lemei Rock area of Skamania County, Washington. The study area is located in the southern part of Washington's Cascade Mountains between 45°54' and 46°07' N. and 121°40' and 121°53' W. This area was selected for study because geologic mapping had identified a north-trending chain of late Quaternary basaltic volcanoes that had extruded a sequence of lava flows up to 600 m thick, and because the chain of volcanoes is areally coincident with a well-defined gravity low with a minimum value of about -110 mgals.

The Quaternary lava flows all exhibit normal remanent magnetic polarity, so are probably less than 690,000 years old. Most of the flows and volcanoes appear to be younger than the Salmon Springs Glaciation (40,000 to 80,000 years ago), and some are younger than Fraser Glaciation (less than about 12,500 years old). One large lava flow (the Big Lava Bed) and its source cinder cone can be shown to be between 450 and 4,000 years old by their relationship to dated ash and cinder deposits erupted from nearby Mount St. Helens. The young basalts rest on deformed Tertiary sedimentary and volcanic rocks. Thermal springs with low discharge and temperatures of less than 50°C occur about 20 km south of the study area.

^{1/} J. Eric Schuster, Department of Natural Resources, Division of Geology and Earth Resources, Olympia, WA 98504.

^{2/} David D. Blackwell, Department of Geological Sciences, Southern Methodist University, Dallas, TX 75275.

^{3/} Paul E. Hammond, Earth Sciences Department, Portland State University, P. O. Box 751, Portland, OR 97207.

^{4/} Marshall T. Huntting, 282 Huntting Road, Silver Creek, WA 98585.

2 HEAT FLOW STUDIES

Gradients of 52.7 and 53.4°C/km and heat flows of 1.8 and 1.6 $\mu\text{cal}/\text{cm}^2\text{sec}$, respectively, were measured in two drill holes near the east flank of the chain of volcanoes. Gradients of 44.5 and 58°C/km and heat flows of 1.3 and 1.6 $\mu\text{cal}/\text{cm}^2\text{sec}$, respectively, were measured in two holes near the axis of the chain, and one gradient of 49.8°C/km and heat flow of 1.5 $\mu\text{cal}/\text{cm}^2\text{sec}$ were measured in a drill hole near the west flank of the chain. All gradients and heat flows are terrain corrected.

These heat-flow values are typical regional heat-flow values for the Cascade Mountains. The data show that there is no large-sized heat source body within the general area of the heat-flow study. However, there is only one location in Washington, also in the Cascade Mountains, where higher gradients have been measured.

INTRODUCTION

Abundant recent volcanic features indicate that the Cascade Range of northern California, western Oregon, and western Washington is one of the major geothermal provinces of the United States. Smith and Shaw (1975) tentatively identified 53 possible active igneous systems in the western United States. Of these systems, 19 (over one-third of the total) are in the Cascade Range. Therefore, investigation of the geothermal characteristics of the Cascade Range is of great importance to the regional resource assessment of the geothermal potential of the western United States, and to the understanding of the geologic controls on, and distribution of, geothermal systems in the Cascades. Understanding the controls on geothermal features in the Cascade Range has an even wider significance because there are many analogous areas around the world. The tectonic setting of the Cascade Range is analogous to the subduction-zone-associated island arc tectonism and volcanism (Atwater, 1970; Blackwell, 1971) so typical of the Pacific Basin.

Quaternary volcanic activity in the Cascades has occurred in two contrasting settings. The most prominent parts of the Pleistocene and Recent volcanic section are the large andesitic stratovolcanoes. These volcanoes make up most of the "identified volcanic systems" listed by Smith and Shaw (1975).

In addition to the andesitic volcanoes, which actually have associated ash deposits and lava flows with compositions ranging from basalt to rhyolite or rhyodacite, there are volcanic centers composed predominantly of basalt. According to Smith and Shaw (1975), there are 34 basaltic lava fields in the conterminous western United States characterized by lava flows less than 10,000 years old; seventeen of these are in the Cascade Range. Although more is known about the andesitic stratovolcanoes, the basalts may be much more abundant volumetrically. According to McBirney and others (1974) the volume of Pliocene and Quaternary basaltic lavas extruded in a portion of the Oregon Cascades, located between 44° and 45° N. and 118° and 124° W., is 3,500 km³ or greater. On the other hand, the volume of andesitic and more silicic volcanic rocks is less than 500 km³. The initial relative volume of magmas involved and the fraction remaining underground as intrusives are, of course, unknown factors; the relative volumes of silicic and basaltic intrusive rocks may well be the reverse of the volumes of silicic and basaltic rocks extruded on the earth's surface.

The known hydrothermal convection systems of the western United States are discussed by Renner, White, and Williams (1975). Of a total of 60 hydrothermal convection systems with subsurface tempera-

tures in excess of 150°C in the conterminous western United States, only 7 are located in the Cascade Range. Of almost 200 systems with temperatures between 90° and 150°C, only 10 are found in the Cascade Range.

Thus, compared to the remainder of the western United States, it appears that the Cascade Range has a higher relative occurrence of volcanic centers than it does of hydrothermal convection systems. This lack of association of hydrothermal convection systems with the youngest volcanic rocks in a given region is also characteristic of the Japanese island arc geothermal systems. Hydrothermal convection systems there are not typically associated with the youngest stratovolcanoes (Yuhara, 1974). It is only after significant erosion has breached the carapace of the volcano that hydrothermal systems are observed. There may be hydrothermal systems present before erosion, but if so, they do not usually have surface manifestations.

Other factors may contribute toward the apparent lack of hydrothermal systems in the Cascade Range as well. The heavy rainfall characteristic of the western parts of the Cascade Range may lead to shallow hydrologic conditions that mask deep geothermal systems, or the systems may not have developed yet. Thus, in order to understand the geothermal systems associated with the suite of rocks of the Cascades, and in order to assess the geothermal potential of the Cascade Range, detailed studies of the volcanic centers and of the regional geothermal characteristics are necessary.

It is generally assumed that silicic volcanic centers are more favorable for development of geothermal systems than basaltic centers (Combs and Muffler, 1973; Smith and Shaw, 1975). However, Smith and Shaw point out that the frequent association of silicic domes with basalt lava fields suggests that such an assumption should be viewed very care-

fully. Most of the silicic centers in the Cascades consist of the young stratovolcanoes and their satellite vents. In general, these centers are in national parks or wilderness areas, surrounded by rugged terrain with poor access where geophysical exploration is very difficult, expensive, and time consuming. In Washington the Quaternary volcanic centers are the andesitic stratovolcanoes—Mount Baker, Glacier Peak, Mount Rainier, Mount St. Helens, and Mount Adams—and the basaltic centers are Indian Heaven fissure zone area, King Mountain fissure zone area, and the Simcoe Mountains area. The basaltic centers are all in the southern part of Washington's Cascade Range.

The Indian Heaven basalt field lies between the stratovolcanoes of Mount St. Helens and Mount Adams in southwestern Washington. The basalts cover an area of 2,200 km² and the youngest flows are no older than 4,000 years. The geology has been studied in detail by Hammond and others (1976) and a gravity survey of the area was done by Stricklin (1975). Because of the greater extent of knowledge about this particular volcanic field, its good accessibility by road, and geothermal leasing interest, the Indian Heaven area was selected as a test area for investigating the geothermal systems of the State of Washington, and of the Cascade Range in general. The geothermal potential of the area was evaluated by drilling a number of heat-flow holes, sited with careful consideration of the available geologic and gravity data. The primary object of this report is to describe the results of those heat-flow studies.

ACKNOWLEDGMENTS

We wish to thank Charles Pezzotti, editor of the Proceedings of the Second United Nations Symposium on the Development and Use of Geothermal

4 HEAT FLOW STUDIES

Resources, for permission to use portions of the report by Hammond and others (1976) in our sections on geology and geophysics. The United States Forest Service was very cooperative during the drilling of heat-flow holes in the Gifford Pinchot National Forest, and we particularly wish to thank Barry Wheeler of the Mount Adams Ranger District for his interest in and assistance with the drilling project. Z. F. Daneš and Claude Stricklin of the University of Puget Sound provided data and helpful suggestions on the gravity of Washington's southern Cascades. The heat-flow research was supported by National Science Foundation Grant AER75-02747.

The division of effort during the execution of this study was as follows: J. Eric Schuster was principal investigator, and measured thermal gradients in the completed drill holes. David D. Blackwell assisted with the siting of the drill holes, measured thermal conductivities of rock samples, calculated heat flows, and provided all of the heat-flow interpretations in this report. Paul E. Hammond mapped the geology of the area, assisted with the siting of the drill holes, and provided the geologic and stratigraphic data for this report. Marshall T. Huntting was field manager, described the lithology of core samples from the drill holes, made bottom-hole temperature measurements, and wrote a drilling history for each hole.

GEOLOGY

GENERAL FEATURES

The Cascade Range extends for about 1,000 km, from the Canadian border to Lassen Peak in northern California. The range has been arched and uplifted some 1,000 to 3,000 m, the greater amount

occurring at the northern end, during the late Pliocene and Pleistocene.

The southern Cascades of Washington (fig. 1, table 1) are composed of calc-alkaline volcanic rocks of Tertiary and Quaternary age. The Cenozoic rocks are predominantly pyroxene andesite, followed by basalt, rhyodacite, dacite, and rhyolite, in decreasing order. Strata are formed by lava flows and breccias, lahars (mostly breccias), river-deposited rocks of volcanic origin, and tephra deposits. Several sequences of widespread ash-flow tuff deposits or ignimbrites (for example, the Stevens Ridge Formation) form marker stratigraphic units and structural datum horizons.

The Tertiary rocks are extensively altered and locally zeolitized to the lowest grades of regional metamorphism (Wise 1959, 1961; Fiske, Hopson, and Waters, 1963; Fischer, 1971; and Hartman, 1973). Many irregular zones of hydrothermal alteration, consisting predominantly of silicification and argillization with disseminated base-metal sulfides (Grant, 1969), are associated with Tertiary plutons. These zones occur mostly outside of the area shown in figure 1, but since the alteration affects all except the most recent strata, presumably geothermal activity has been a common phenomenon in the southern Cascades of Washington for much of the Cenozoic Era.

Quaternary basalts have been erupted onto the Tertiary rock units, which were previously folded and faulted. Most faults in the southern Cascades of Washington trend northwest or north and are normal faults. Movement on some was as late as Quaternary. Folds are usually rather broad and open; in the northern part of the area, they trend west or northwest, and in the southern part southwest. The Quaternary basalts are not folded.

The crestal part of the range, including the Indian Heaven fissure zone area (fig. 1) is deeply

TABLE 1.—Cenozoic geologic units of the southern Cascade Range, Washington

Age	Map symbol	Unit	References	Lithology	Thickness (m)	
QUATERNARY	Qhv	Volcanic rocks of Mount St. Helens	Hopson (1971), Crandell and Mullineux (1973)	Chiefly pyroxene andesite, dacite, and olivine basalt lava flows and breccia, mudflow and pyroclastic flows, and tephra deposits	10 to 250	
		Volcanic rocks of Mount Adams	Sheppard (1967), Hopkins (1969, 1976)	Mainly olivine, hypersthene-augite, and hornblende andesite porphyry lava flows and breccia, mudflow and pyroclastic flows, and tephra deposits	10 to 200	
			unconformity			
	Qb	Basalts of fissure zones (includes basalts of Trout Creek Hill and Big Lava Bed of Wise, 1970, and Waters, 1973, Camas Prairie and White Salmon River of Sheppard, 1964)	Hammond (1973), Pedersen (1973)	Pahoehoe to blocky olivine and/or pyroxene basalt lava flows, breccia, scoria, and cinder deposits	1 to 60	
				unconformity		
	Qc	Andesite near Laurel (includes brecciated rhyolite of Mann Butte)	Sheppard (1964)	Augite-hornblende andesite lava flows and breccia	10 to 250	
				unconformity		
	Pliocene-Pleistocene	QTb	Miscellaneous basalts of Sheppard, 1964, Newcomb, 1969, and Wise, 1970	Waters (1973)	Olivine basalt lava flows, breccia, scoria, cinders, and pillow-palagonite breccia	1 to 100
					unconformity	
		QTa	Andesites of Soda Peak and Timbered Peak (includes miscellaneous andesites of Sheppard, 1964)	Wise (1970)	Olivine-hypersthene-hornblende andesite lava flows, breccia, and cinder deposits	20 to 100
TERTIARY	Ty	Yakima Basalt (includes Ellensburg Formation of Sheppard, 1964, and Newcomb, 1969)	Sheppard (1964), Newcomb (1969), Holmgren (1969), Wise (1970), Waters (1973)	Dark-colored basalt flows and pillow-palagonite breccia; light-colored tuffaceous, diatomaceous siltstone, sandstone, and conglomerate interbeds	100 to 600	
				regional unconformity		
	Tec	Eagle Creek Formation	Wise (1970), Waters (1973)	Light-colored, well-bedded volcanic conglomerate, mudflow breccia, sandstone, tuff; few pyroxene andesite and basalt lava flows	80 to 1000	
				unconformity		
	Tv	Pre-Eagle Creek volcanic and sedimentary rocks	Harle (1974)	Dark-colored pyroxene andesite and basalt lava flows and breccia, mudflow, and volcanic sedimentary rocks	400	
	Tsr	Stevens Ridge Formation	Fiske, Hopson, and Waters (1963), Hammond (1974)	Light-colored tuff, pumice, and lithic breccia; volcanic sedimentary rocks; few basalt, andesite, and silicic lava flows and breccia	90 to 600	
				regional unconformity		
Eocene-Oligocene	To	Ohanapocosh Formation	Fiske, Hopson, and Waters (1963), Wise (1970), Waters (1973)	Interstratified dark-colored basalt and pyroxene andesite lava flows and breccia, and varicolored andesite to rhyodacite pyroclastic and volcanic sedimentary rocks	4500 Base not exposed	

6 HEAT FLOW STUDIES

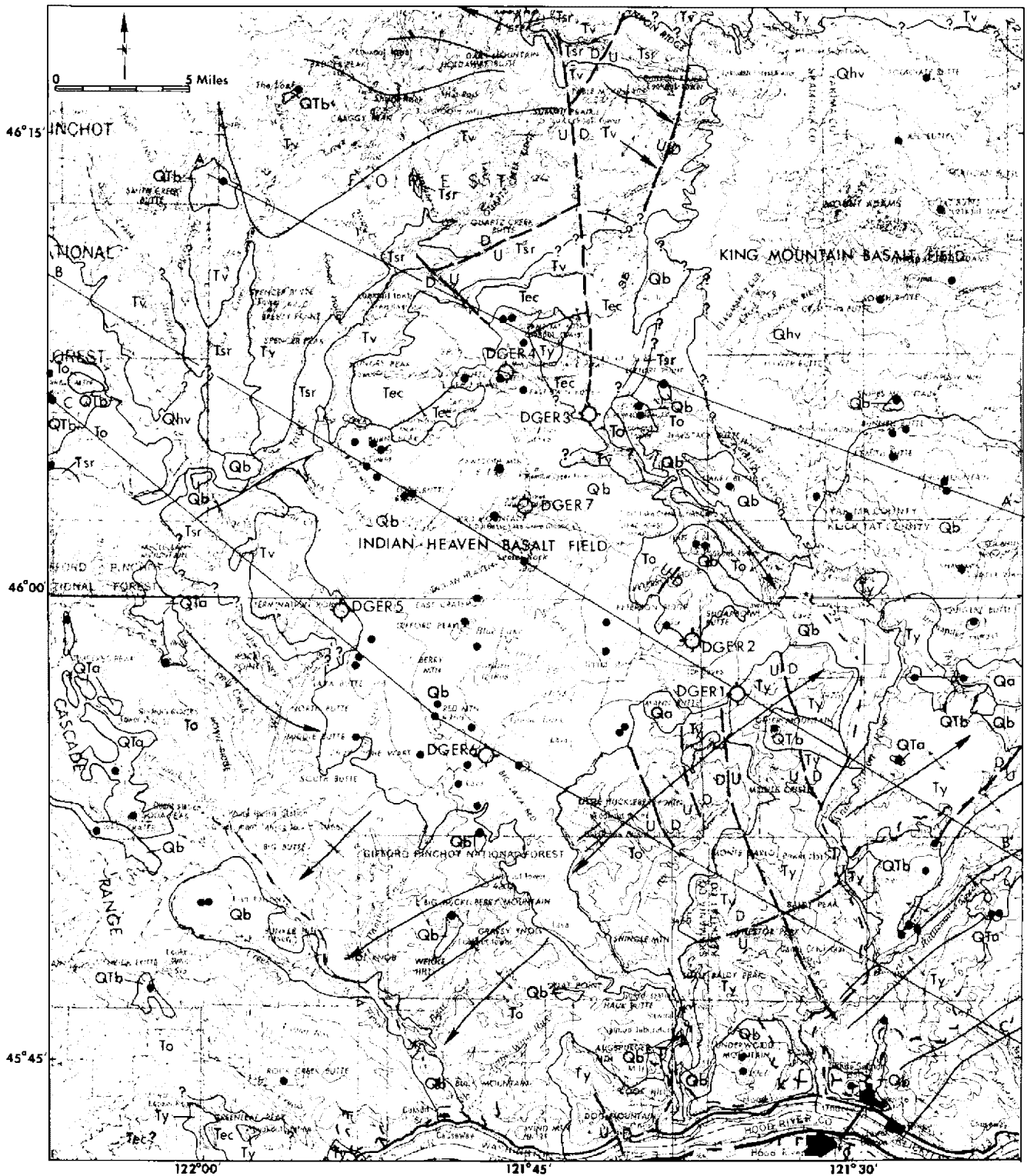
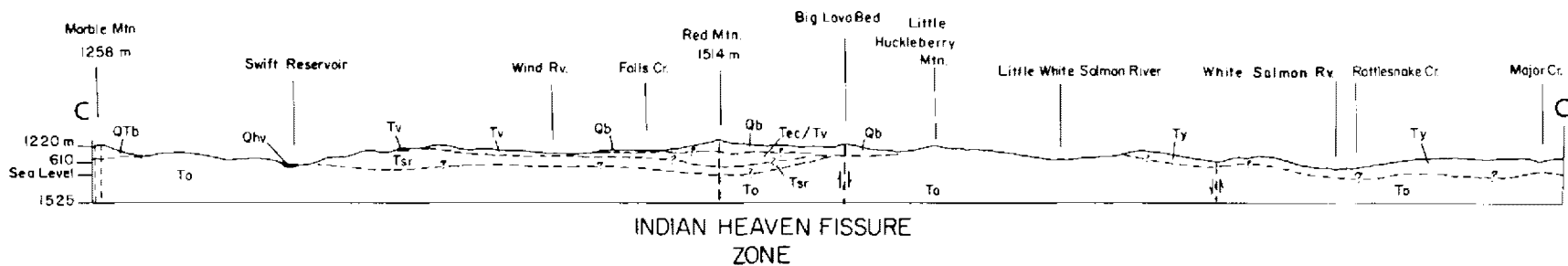
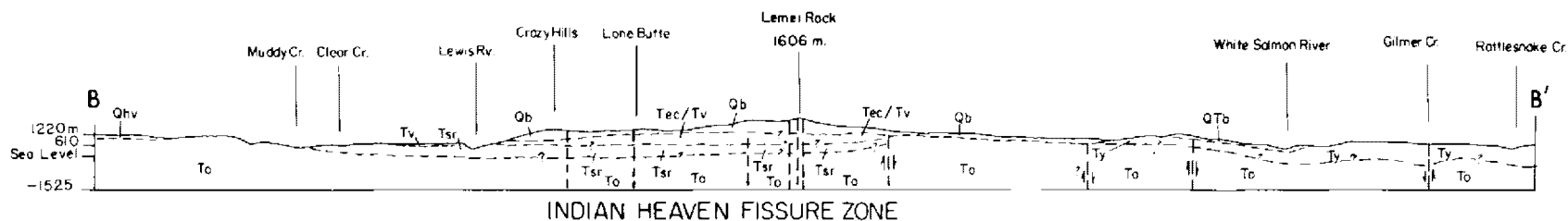
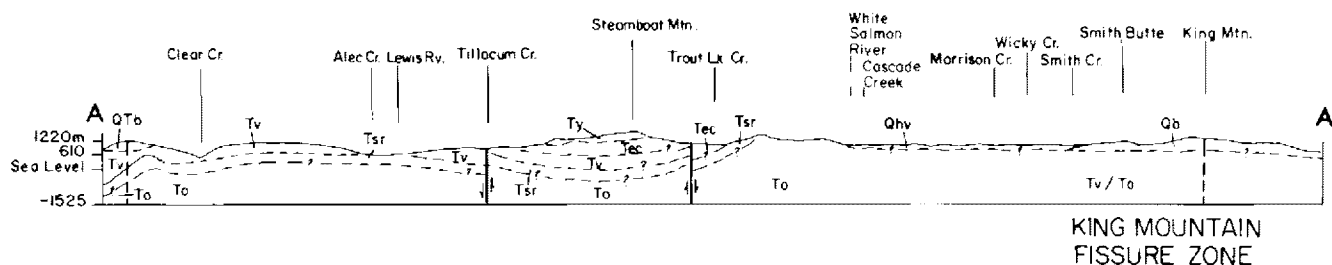


FIGURE 1.—Generalized geologic map and cross sections of part of the southern Cascade Range, Washington (for explanation of geologic units, see table 1).

MAP EXPLANATION

- ?— Contact, queried where indefinite
- ?--- Fault, queried where indefinite
- ←?— Trace of anticlinal axis, showing direction of plunge, queried where indefinite
- ←?— Trace of synclinal axis, showing direction of plunge, queried where indefinite
- Volcanic center
- ⊙ DGER 2

CROSS SECTIONS



8 HEAT FLOW STUDIES

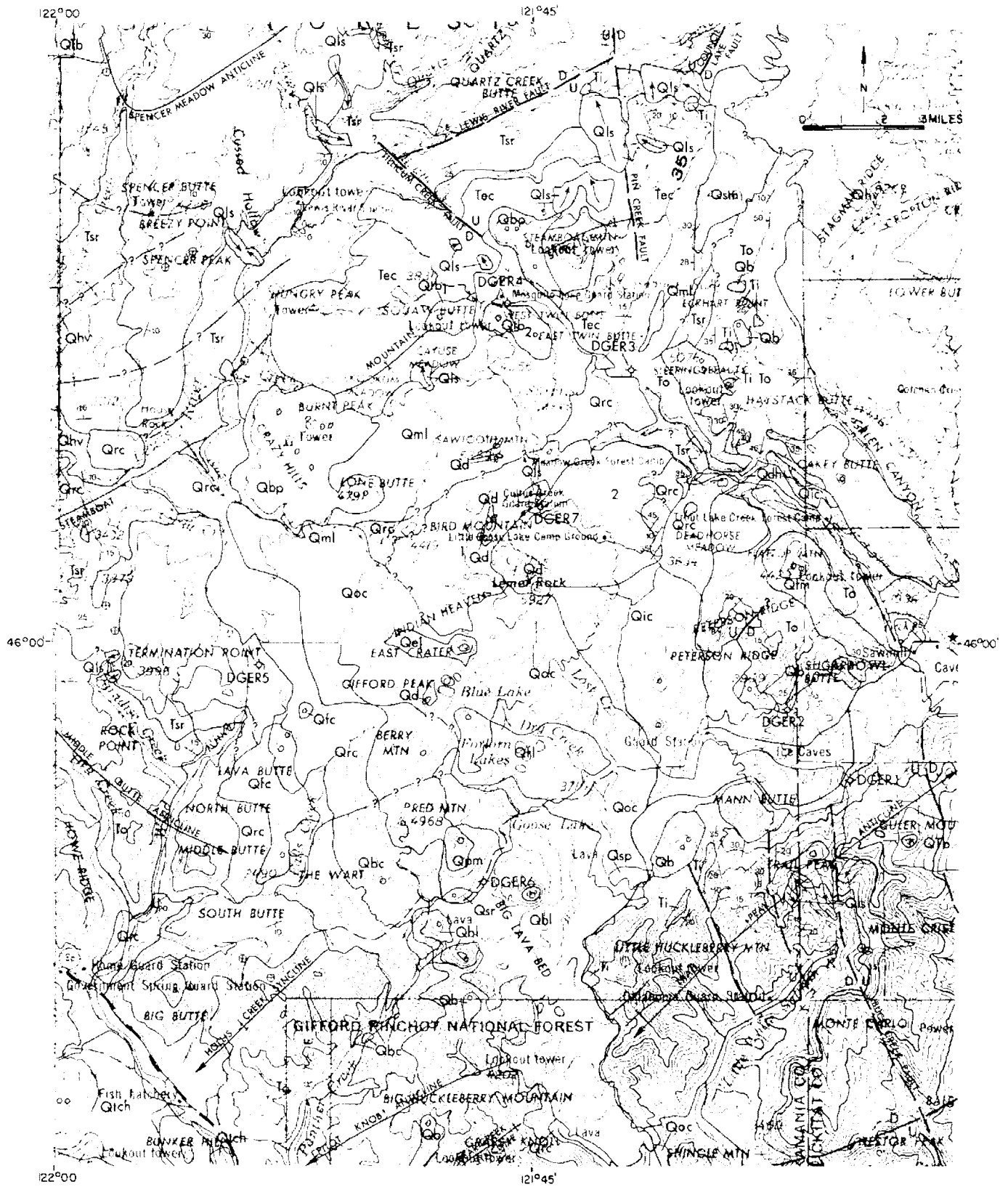


FIGURE 2.—Geologic map of the Indian Heaven area, southern Cascade Range, Washington.

EXPLANATION

	<u>EXTRUSIVE AND SEDIMENTARY ROCKS</u>	<u>INTRUSIVE ROCKS</u>	
QUATERNARY	Qls Landslides		QUATERNARY
	Qlv Volcanic rocks, mostly andesites, of Mount St. Helens and Mount Adams		
	Qbl Basalt of the Big Lava Bed		
	Qsr Cinders of South Red Mountain		
	Qtb₁ Basalt, younger, of Twin Buttes		
	Qtb₂ Basalt, older, of Twin Buttes		
	Qbp Basalt and pillow palagonite of Burnt Peak		
	Qic Basalt of Ice Cave		
	Qsm Basalt of Swampy Meadows		
	Qel Basalt of Eunice Lake		
	Qfc Basalt of Falls Creek		
	Qfl Basalt of Forlorn Lakes		
	Qpm Basalt of Papoose Mountain		
	Qbc Basalt of Black Creek		
Qfm Basalt of Flattop Mountain			
Qoc Basalt of Outlaw Creek		TERTIARY	
Qsp Basalt of South Prairie			
	Qd Basaltic dikes and plugs (Pleistocene)		
			MIOCENE- PLEISTOCENE
			Qrc Basalt of Rush Creek
			Qrch Basalt of Trout Creek Hill
			Qml Basalt of Mosquito Lake
			Qdh Basalt of Deadhorse Creek
			Qld Basalt, undifferentiated, of Little Deer Point
			Qld₁ Basalt, younger, of Little Deer Point
			Qld₂ Basalt, older, of Little Deer Point
			Qb Basalts, less than 690,000 years old
			Qa Andesites, less than 690,000 years old, includes brecciated rhyolite of Mann Butte
			Qtb Basalts, greater than 690,000 years old
		Ty Yakima Basalt, and associated sedimentary rocks	
		Tec Eagle Creek Formation	
		Tv Pre-Eagle Creek volcanic and sedimentary rocks	
		Tsr Stevens Ridge Formation	
		To Ohanapecoh Formation	
		Ti Hypabyssal intrusive rocks (Miocene or younger)	

- | | |
|--|--|
| <p>— ? — Contact, queried where indefinite</p> <p>— ? - - - Fault, hachures on downthrown side, queried where indefinite</p> <p>← ? — Trace of anticlinal axis, showing direction of plunge, queried where indefinite</p> <p>← ? — Trace of synclinal axis, showing direction of plunge, queried where indefinite</p> <p>○ Volcanic center</p> | <p>— 45° Strike and dip of strata</p> <p>⊕ Horizontal strata</p> <p>⊕ Drill hole locations</p> |
|--|--|

dissected by glaciation. Consequently, large areas are mantled by till and glacial outwash deposits. In other areas, a thick soil cover has been developed.

CENOZOIC ROCKS

Tertiary stratigraphic units are summarized in table 1. The oldest rocks exposed are part of the Ohanapecosh Formation, of Eocene-Oligocene age. The strata are over 4,500 m thick and consist of interstratified volcanic sediments, andesite and basalt lava-flow complexes, and debris-flow breccias. Individual units are well-stratified but discontinuous laterally, and marker or traceable strata are lacking.

The Ohanapecosh is overlain unconformably by the major Tertiary marker unit, the Stevens Ridge Formation, which is largely ash-flow tuffs and interbedded volcanic sedimentary rocks, and from 90 to 600 m thick. The Stevens Ridge Formation is Miocene in age; it was radiometrically dated at 20 to 25 million years old by Hartman (1973). The Stevens Ridge Formation is overlain conformably by pre-Eagle Creek volcanic and sedimentary rocks, composed of pyroxene andesite lava flow complexes and volcanic sediments, with a maximum thickness of 400 m.

The Ohanapecosh and Stevens Ridge Formations and the pre-Eagle Creek volcanic and sedimentary rocks can be traced almost continuously through the area (fig. 1). Of the three formations, Ohanapecosh and Stevens Ridge rocks are considered the least permeable, the former because of widespread zeolitization, and the latter because of its compactness, zeolitization, and high clay content. The three units may be highly permeable in fault or fracture zones, and the pre-Eagle Creek volcanic and sedimentary rocks may be moderately permeable because of interstratified lava flows, breccias, and sediments.

The Eagle Creek Formation, which unconformably overlies older strata and is up to 1,000 m thick, is composed of volcanic sediments, conglomerate, debris-flow breccia, and minor lava flows. It contains permeable beds, which may constitute a possible groundwater reservoir beneath the northern end of the Indian Heaven fissure zone.

Basalt of the Columbia River Group, of Miocene age, occurs in a small area within the Cascade Range at Steamboat Mountain and also occurs along the eastern margin of the range and extending eastward toward the Columbia Basin. South and east of Mount Adams, the basalt forms structural ridges, basins, and upland plateaus.

During the uplift of the Cascade Range, upper Pliocene or lower Quaternary olivine-hypersthene-hornblende andesite lavas, breccias, and cinder deposits were erupted. These rocks are restricted in areal extent and form strata no more than 100 m thick. All of these lavas tested so far have reversed remanent magnetic polarity. Principal occurrences are at Soda Peak and Timbered Peak (fig. 1).

Pliocene or Quaternary olivine basalt lavas, breccias, and cinders, believed to be older than 690,000 years based on their reversed remanent magnetic polarity and degree of erosional dissection, occur in several places. These basalts form volcanoes west of Wind River and near Mount St. Helens.

The oldest Quaternary rock unit in the area is an andesite volcano near Laurel (Sheppard, 1964), east of the White Salmon River, that has normal remanent magnetic polarity. A younger group of olivine basalts, from 690,000 years old to possibly as young as 450 years based on normal remanent magnetic polarity and interstratified relationships with dated tephra deposits erupted from Mount St. Helens, compose the basalt fields of the Indian Heaven and King Mountain fissure zones (fig. 1). The Quaternary

basalts of the Indian Heaven fissure zone are the rocks of primary interest in this report (fig. 2).

Volcanic deposits, composed of lavas, breccias, tephra, mudflows, and pyroclastic flow deposits up to 250 m thick and younger than 690,000 years old, form Mount St. Helens and Mount Adams stratovolcanoes.

QUATERNARY BASALTS

The Quaternary basalts were extruded from two parallel north-trending fissure zones lying about 25 km apart (fig. 1). The east fissure, called the King Mountain fissure zone, extends from Quigley Butte and King Mountain northward beneath Mount Adams to Walupt Lake volcano, a distance of 48 km. At least 10 lava groups (fig. 2, table 2) arising from eight volcanic centers have been recognized and mapped in this zone.

The western zone, called the Indian Heaven fissure zone, extends from Red Mountain 30 km northward to the cones on the west ridge of Steamboat Mountain (fig. 2). Two small intraglacial basaltic cones, near the Cispus River about 22 km north of Steamboat Mountain, constitute a possible extension of the fissure zone. Major volcanoes are East Crater, the source of a group of lavas traceable on both flanks of the zone, and Lemei Rock, the source of an extensive flow (basalt of Ice Cave), which descended into the White Salmon River valley. At least 14 groups of lava flows have been mapped along the Indian Heaven zone (fig. 2, table 2).

All volcanic centers are shown on figure 1. A number of the volcanic centers are not aligned with the fissure zones, indicating the existence of flanking or subsidiary structural zones along which some recent volcanic eruptions took place (West Crater, for example).

The fissure zones cannot be traced into well-defined, north-trending faults or graben extending

along the crest of the range, nor do they align southward with the Hood River graben across the Columbia River in Oregon (Allen, 1966, p. 21-23). Some isolated volcanoes appear to lie along northwest-trending faults. The alignment of West Crater and Trout Creek Hill volcanoes with the lower Wind River and St. Martin Hot Springs may be evidence of a fault. The southwest-trending folds east of the Wind River, which cannot be traced across the Wind River valley, give further support to the existence of a fault in the valley.

Each volcanic center consists of a shield volcano surmounted by one or more cinder cones. Where the volcanoes have been deeply glaciated, such as at Sawtooth (fig. 4) and Bird Mountains (fig. 2), bedded cinders, narrow ridges of lavas dipping outward in all directions, and interlacing narrow dikes of basalt and breccia forming the skeletal framework of the volcanoes can be delineated.

The lava flows can be mapped in the field on the basis of differences in phenocrystic minerals and stratigraphic and topographic positions. Many lavas can be traced from complex broad flank sheets into intracanyon flows. Most lavas are pahoehoe and, at the time of extrusion, were highly fluid. Individual flows range from 1 to 50 m thick, the average being 2 m in thickness. They have vesicular to scoriaceous bases and vesicular to slab pahoehoe tops. Jointing is blocky to slabby; only in the thicker intracanyon flows is columnar jointing well developed. Contacts are rarely exposed except in valleys that were incised after the last glaciation. Fluvial sedimentary interbeds form locally well-stratified to cross-bedded units up to 4 m thick. The lava sequence forms highly permeable strata.

All fresh flow rocks are colored shades of gray; some are oxidized locally to shades of brown. Most are dense, completely crystalline, and rarely inflated. Olivine or olivine and pyroxene phenocrysts

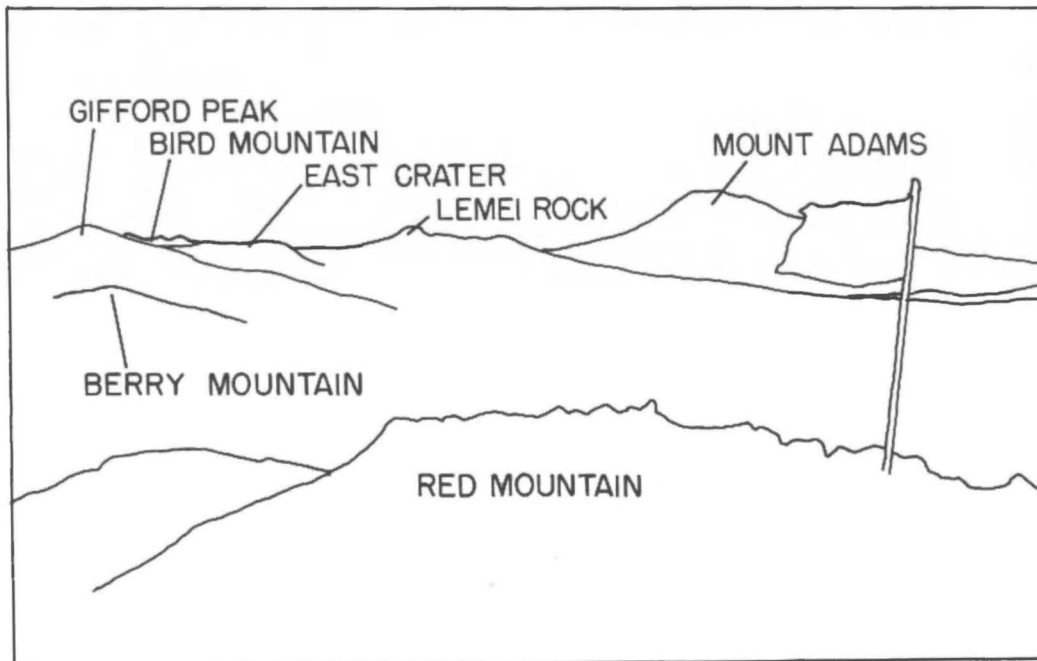
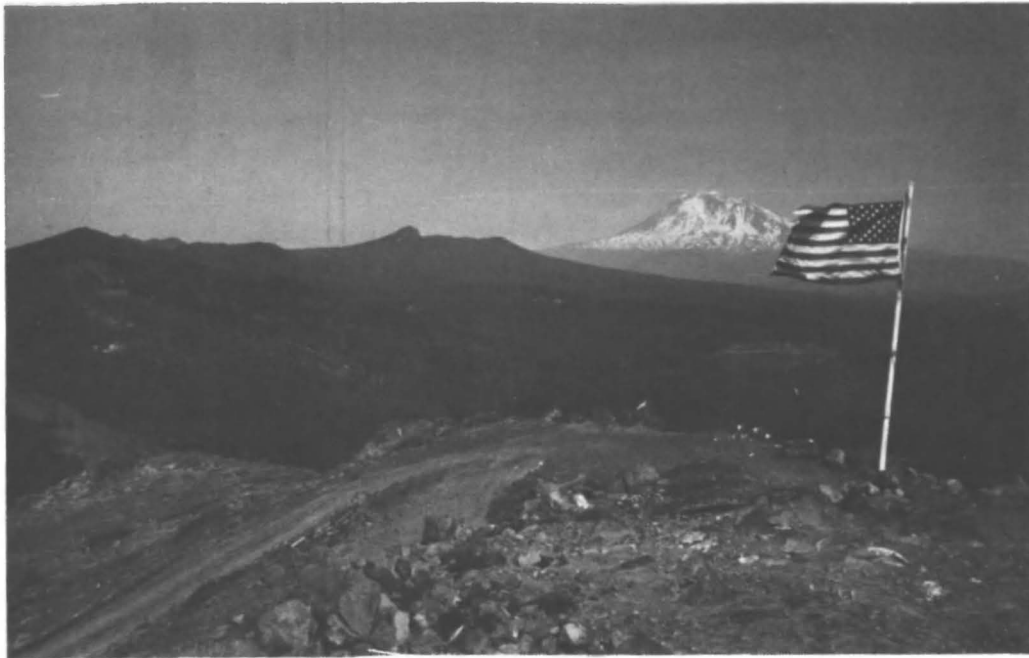


FIGURE 3.—View to the north from Red Mountain.

TABLE 2.—Quaternary basalts and interbedded cinders and ash in a portion of the southern Cascade Range, Washington^{1/}

Age (years before present)	Unit	Symbol (on fig. 2)	Source	Description	Total thickness (ft)
Indian Heaven fissure zone					
450 to 1,150	"W" tephra set	Not shown	Mount St. Helens
	Basalt of the Big Lava Bed	Qbl	Dark-gray basalt, 10 percent very fresh olivine phenocrysts, vesicular to dense, slab pahoehoe to scoriaceous top, tumuli and pressure ridges, flows 5 to 30 ft thick (Wise, 1970, p. 32-33; sample localities 19 and 20)	100 to 300
3,000 to 4,000 6,600	Cinders of South Red Mountain	Qsr
	"V" tephra set	Not shown	Mount St. Helens
8,000 to 12,000 12,000 to 18,000 ca. 12,500	"O" ash	Not shown	Mount Mazama (Crater Lake)
	Basalt of West Crater	Not shown	West Crater	Gray basalt, 5 percent porphyritic olivine, dense, blocky, flows 10 to 15 ft thick (Wise, 1970, p. 33)	100 to 200
ca. 20,000	Basalt of Twin Buttes	Qtb ₁ Qtb ₂	Snow Butte Twin Buttes	Gray olivine basalt, vesicular to dense, blocky to scoriaceous, flows 10 to 30 ft thick	100 to 400
	"J" Tephra set	Not shown	Mount St. Helens
ca. 20,000	"S" Tephra set	Not shown	Mount St. Helens
	End of Fraser Glaciation (Evans Creek and Vashon Stades of Crandell and Miller, 1974)
ca. 20,000	Basalt and pillow palagonite of Burnt Peak	Qbp	Crazy Hills, Lone Peak, west ridge of Steamboat Mountain	Gray olivine basalt, vesicular to dense, blocky, forms pillow-palagonite breccia, flows 30 to 150 ft thick (Pedersen, 1973)	100 to 1,000
	Beginning of Fraser Glaciation
ca. 20,000	Basalt of Ice Cove	Qic	Lemei Rock	Gray basalt, 10 percent glomeroporphyritic olivine, 25 percent tabular plagioclase, vesicular, slab pahoehoe to scoriaceous top, scoriaceous base, flows 5 to 30 ft thick (Sheppard, 1964, olivine basalt of White Salmon River)	5 to 100
	Basalt of Eunice Lake	Qel	East Crater	Gray olivine basalt, dense, blocky, flows 10 to 30 ft thick	10 to 100
ca. 20,000	Basalt of Falls Creek	Qfc	West of Berry and Red Mountains	Light-gray basalt, dense, platy to slabby, flows 30 to 100 ft thick (Wise, 1970, sample locality 29)	30 to 200
	Basalt of Forlorn Lakes	Qfl	Southeast of Gifford Peak	Light-gray basalt, dense, platy to slabby, flows 30 to 100 ft thick (Wise, 1970, sample locality 32)	30 to 400
ca. 20,000	Basalt of Passaic Mountain	Qpr	Gray basalt, 15 percent porphyritic olivine, dense, blocky, flows 10 to 30 ft thick	10 to 300
	Basalt of Black Creek	Qbc	Red Mountain	Gray olivine basalt, dense, blocky, flows 10 to 30 ft thick (Wise, 1970, p. 31; sample locality 23)	10 to 400
ca. 20,000	Basalt of Flattop Mountain	Qfm	Gray olivine basalt, vesicular to dense, blocky, flows 10 to 30 ft thick	10 to 150
	Basalt of Outlaw Creek	Qoc	East Crater, Gifford Peak, and/or Lemei Rock	Dark-gray olivine basalt, vesicular to slightly inflated, blocky and scoriaceous, flows 5 to 20 ft thick (Wise, 1970, sample locality 18)	5 to 200
ca. 20,000	Basalt of South Prairie	Qsp	Dark-gray olivine basalt, vesicular, scoriaceous, flows 5 to 20 ft thick	5 to 30
	Basalt of Rush Creek	Qrc	Gifford Peak or Berry Mountain	Gray basalt, 10 percent glomeroporphyritic olivine, 25 percent tabular plagioclase, vesicular to dense, flows 5 to 30 ft thick	5 to 600
ca. 20,000	Basalt of Trout Creek Hill	Qrch	Dark-gray basalt, 20 percent glomeroporphyritic olivine, vesicular to dense, blocky, flows 5 to 30 ft thick (Wise, 1970, p. 32; sample localities 25 and 26; Waters, 1973)	5 to 150
	End of Salmon Springs Glaciation
ca. 20,000	Basalt of Mosquito Lake	Qml	Sawtooth Mountain	Gray olivine basalt, dense, platy to blocky, flows 10 to 20 ft thick	10 to 150
	Beginning of Salmon Springs Glaciation
ca. 20,000	Basalt of Deadhorse Creek	Qdh	Bird Mountain(?)	Gray basalt, 5 percent porphyritic olivine, 5 percent hypersthene, 20 percent plagioclase, dense, blocky, flows 10 to 30 ft thick	30
	Basalt of Little Deer Point	Qld	Bird Mountain or Lemei Rock	Gray olivine basalt, dense, blocky, flows 10 to 100 ft thick	10 to 350
King Mountain fissure zone					
ca. 12,500-20,000	Fraser Glaciation
	Basalt of Swampy Meadows	Qsm	Beneath Mount Adams	Gray olivine basalt, vesicular to dense, blocky, flows 10 to 30 ft thick	10 to 150

^{1/} Only those units shown on figure 2 are described.



FIGURE 4.—Sawtooth Mountain, looking toward the northeast.

are common. Olivine content is variable. Two flows are noted for their abundant platy plagioclase phenocrysts. One, basalt of Rush Creek, flowed from Gifford Peak or Berry Mountain into the Lewis and Little White Salmon River valleys; another, the basalt of Ice Cave (basalt of White Salmon River, Sheppard, 1964) flowed from Lemei Rock volcano down the White Salmon River valley. These two flows are separated stratigraphically by a number of smaller, less extensive flows, characterized by few to no phenocrysts in a dense matrix. The two flows may indicate episodic voluminous outpourings marking the renewal of fresh fluid magma along the zone.

All of the Quaternary basalts exhibit normal remanent magnetic polarity, indicating a probable

age younger than 690,000 years. Most flows are older than Fraser Glaciation; that is, more than 20,000 years old (Crandell and Miller, 1974). Lava flows of King Mountain are radiometrically dated at 100,000 to 300,000 years old (Kienle and Newcomb, 1973) and are possibly the oldest of the Quaternary basalts. The cones of Smith Butte, Bunnell Butte, and Snipes Mountain are younger than Fraser Glaciation (less than 10,000 years) and older than the Trout Lake mudflow, which is about 5,070 years old (Hopkins, 1976). To the north of Mount Adams, Potato Hill is younger than Fraser Glaciation. Walupt Lake volcano is capped by subglacial basaltic deposits of palagonite tuff and pillow lavas and, therefore, is estimated to be between 10,000 and 20,000 years old.

At the Indian Heaven fissure zone, lavas of Sawtooth and Bird Mountains at the northern end of the zone are the only rocks found so far to be older than Salmon Springs Glaciation, 40,000 to 80,000 years old (Crandell and Miller, 1974). Many flows of the zone post-date Salmon Springs Glaciation and are believed to be between 20,000 and 40,000 years old. Pedersen (1973) considers the intraglacial basalts at Crazy Hills and Lone Butte to be between 14,500 and 20,000 years old. Subglacial deposits of similar age form cones along the west ridge of Steamboat Mountain. Twin Buttes cinder cones, between Steamboat and Sawtooth Mountains, are believed to be slightly younger than Fraser Glaciation, less than about 12,000 years old, because of their minimal glacial dissection. The cinder cone, at the southern base of Red Mountain, and Big Lava Bed (fig. 5), at the southern end of the fissure, are younger than Fraser Glaciation. Their cinder deposits are layered between the "Y" and "W" tephra deposits of Mount St. Helens and are, therefore, between 450 and 4,000 years old (Mullineaux, Hyde, and Rubin, 1975). West of the Indian Heaven fissure zone, lavas of Trout Creek Hill volcano are interstratified between till sheets of the Salmon Springs and Fraser Glaciations. The volcano is believed, therefore, to be between 20,000 and 40,000 years old. Waters (1973) states that the lava is older than 35,000 years, beyond determination by the radiocarbon method. The West Crater flows, northwest of Trout Creek Hill, are interstratified with the "J" tephra deposit of Mount St. Helens and the "O" tephra deposit of Mount Mazama (Crater Lake, Oregon) and, therefore, are between 6,600 and 8,000 years old (Mullineaux, 1974; Mullineaux, Hyde, and Rubin, 1975).

The fissure zones and north-trending faults are subparallel in the area west of Mount Adams. Gravity data suggest that the north-northwest-trending fault just east of Steamboat Mountain continues south-

southwestward beneath the Quaternary basalts along the eastern side of the Indian Heaven zone and dies out to the south. This fault may be the conduit for the Big Lava Bed flow. At the north end of the Indian Heaven zone, the younger Tertiary rock units, Eagle Creek Formation and basalts of the Columbia River Group are preserved in the trough of a syncline. The southern extent of pre-Eagle Creek volcanic and sedimentary rocks and the Eagle Creek Formation in this syncline is not known because of the Quaternary basalt cover.

One anomalous feature is Mann Butte, located between the two zones, which consists of brecciated rhyolite. The butte appears to be the erosional rem-

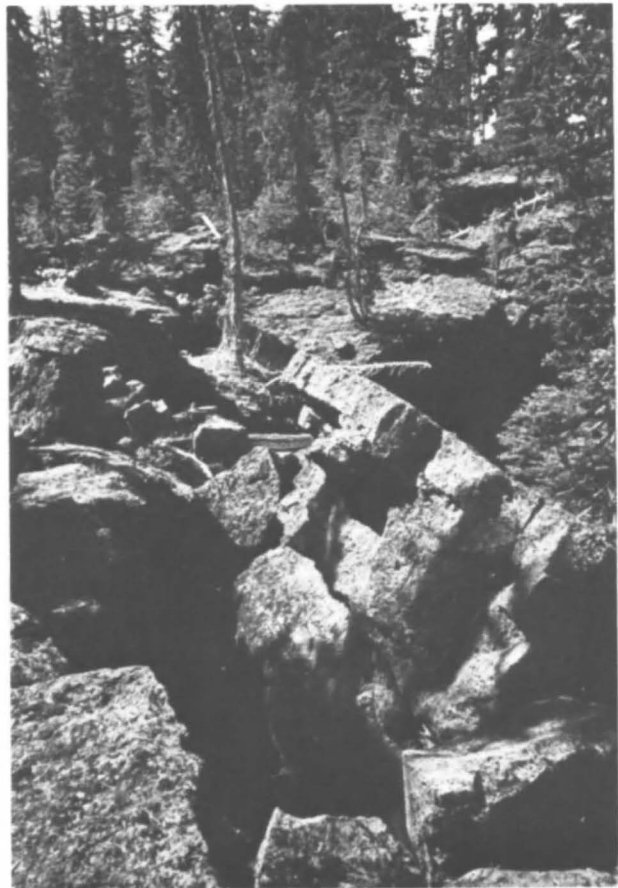


FIGURE 5.—Broken and jumbled basalt blocks at the edge of the Big Lava Bed in the southern part of the study area.

nant of a plug, possibly a protrusion dome. In surficial deposits at its north base is a white clay layer, derived from volcanic ash and pumice, sandwiched between the Salmon Springs and Fraser Glaciation till sheets. If the ash were derived from the dome during its eruptive emplacement, Mann Butte could be as young as late Pleistocene. If it is that young, it constitutes evidence for the presence of silicic magma in the area at about the time of eruption of at least some of the Quaternary basalts.

GEOPHYSICS

Gravity surveys of a large part of the area were performed by Konicek (1974, 1975) and Stricklin (1975), graduate students under the supervision of Z. F. Daneš at the University of Puget Sound. Additional data were obtained from Daneš (written communication, 1973) and from Bonini, Hughes, and Daneš (1974). These gravity data are presented as figure 6. The main gravity feature is a well-defined low of minus 100 mgals coinciding with the Indian Heaven fissure zone. It presents a problem—instead of a low it should be a gravity high, as expected where basalt intrudes less dense sedimentary rocks. Especially perplexing is the position of part of the maximum low, centered in the outlier of basalt of the Columbia River Group at Steamboat Mountain at the northern end of the fissure zone. The anomaly may be due to a thickening of the Tertiary stratigraphic section, especially the Eagle Creek Formation, within the synclinal low at the north end of the fissure zone (a condition similar to the gravity low at Big Butte in the southwestern part of the area); fracturing and brecciation of pre-Quaternary rocks beneath the fissure zone; the presence of a large hydrothermally altered zone beneath the fissure zone; the presence of a shallow magma chamber 1 or 2 km beneath the

surface; or possibly the presence of low-density subglacial volcanic rocks in the Quaternary section at the north end of the fissure zone.

A steep gravity gradient lies along the eastern side of the Indian Heaven fissure zone. Stricklin (1975) suggests that the gradient represents a fault with the east side downdropped a maximum of 2.5 km. If so, the fault might be a continuation of the north-northwest-trending fault mapped just east of Steamboat Mountain.

The area between the fissure zones has a poorly defined relative gravity high. The strongest part of this high, about 25 milligals higher than its surroundings, is partially coincident with a major northeast-trending anticline between the Big Lava Bed and the White Salmon River and may represent a thickened section of denser rocks in the core of the fold.

In light of the condition at the Indian Heaven fissure zone, a gravity low might be expected to be associated with the King Mountain fissure zone. Such is not the case. This suggests that the gravity anomaly at the Indian Heaven fissure zone may not be attributable to the process of extrusion of the Quaternary basalts, since this process should have been similar for both fissure zones.

Detailed airborne magnetic data (fig. 7) became available from the U.S. Geological Survey (1975) during the course of siting the heat-flow drill holes. The magnetic data obviously reflect the presence of the near-surface lava flows of the fissure zones and Mount Adams, but they have not been studied or interpreted with regard to deeper-seated magnetic anomalies.

The Indian Heaven area is on the margin of several published microearthquake surveys (Crosson, 1972, 1974; Unger and Mills, 1973). The results of these surveys suggest that there is more microearthquake activity associated with, and northeast of,

Contour interval 5 milligals. Reduction density 2.67 gm/cm³. Sources of data, Stricklin 1975, Konicek 1974, 1975, Daneš 1973, Bonini, Hughes, and Daneš 1974.

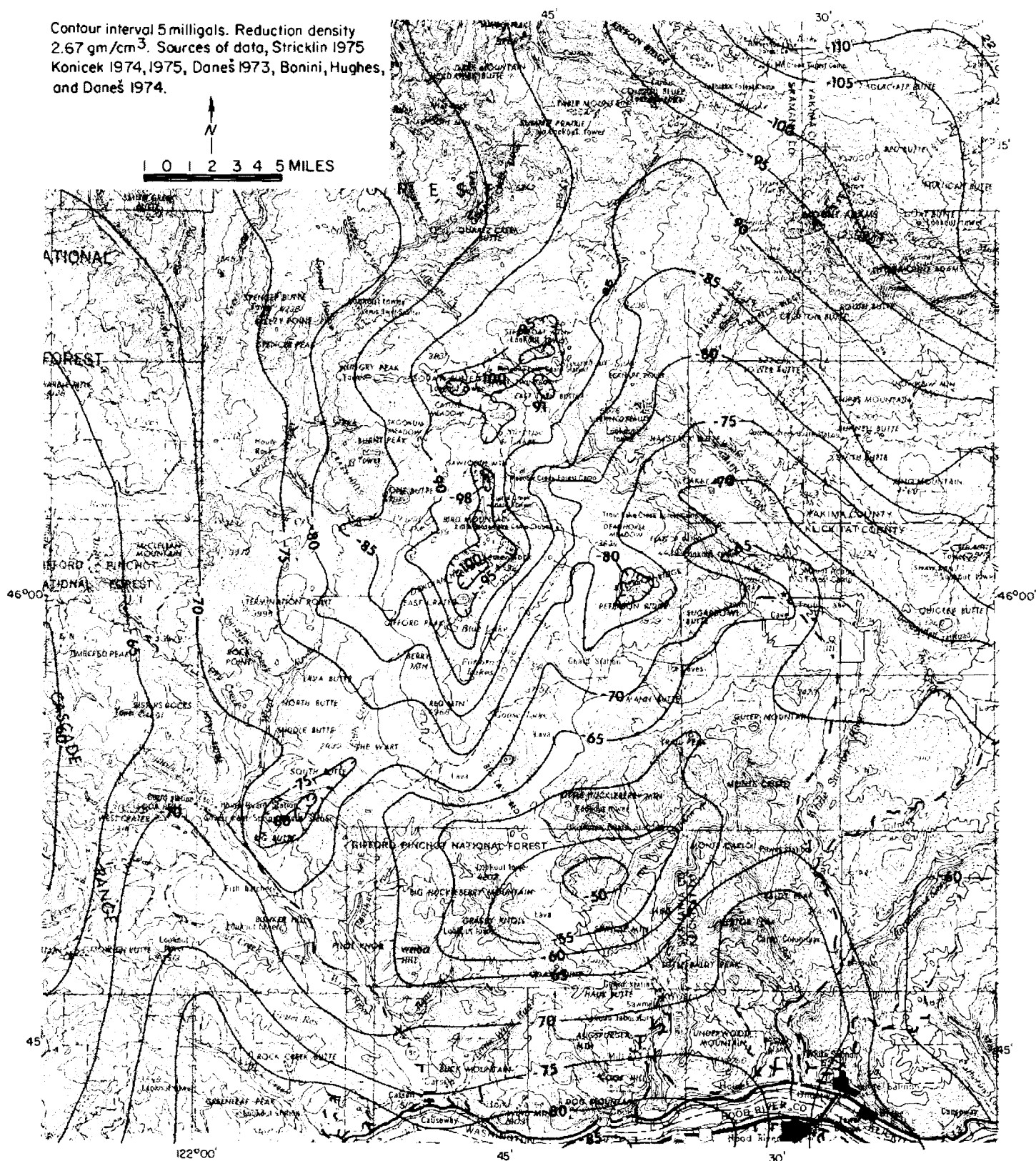


FIGURE 6.—Bouguer gravity map of part of the southern Cascade Range, Washington.

18 HEAT FLOW STUDIES

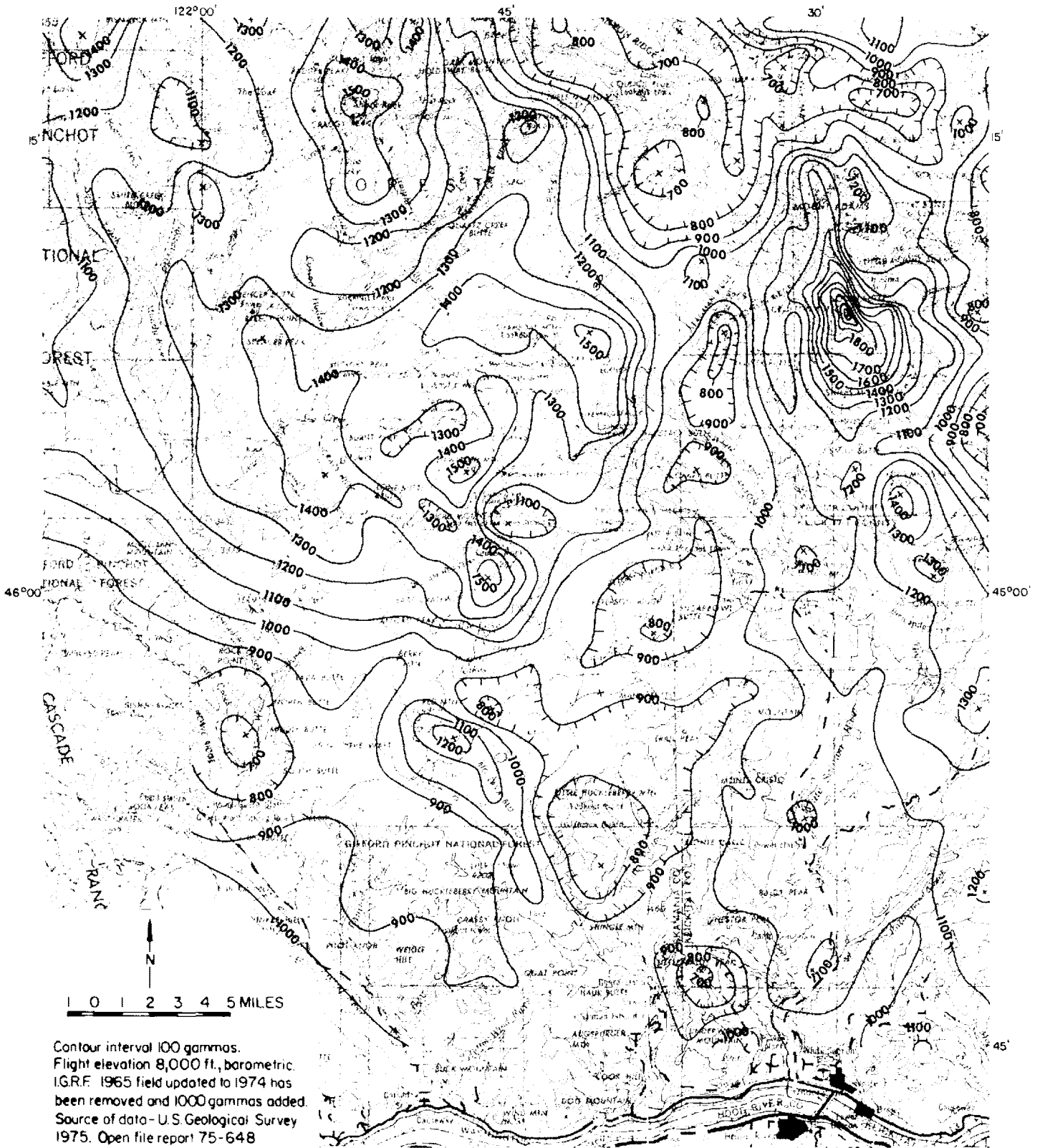


FIGURE 7.—An aeromagnetic map of part of the southern Cascade Range, Washington.

Mount St. Helens than with Mount Adams or the intervening Indian Heaven area. Because the instrumental arrays used in the published surveys were at rather long range from the Indian Heaven area and micro-earthquakes are difficult to detect at long range, it would be desirable to have microearthquake surveys located nearer to the Indian Heaven area.

GEOCHEMISTRY

Chemical data for thermal and mineral springs, cold springs, and some river waters in the Washington Cascades are presented in table 3 and sample locations are shown on figure 8. Many of these data were previously published by Schuster (1974), and Gizienski, McEuen, and Birkhahn (1975), but additional analyses for river waters are presented here.

Predicted source temperatures calculated from the abundance of certain chemicals in spring waters are very useful because they can provide an indication of the geothermal potential of an area at low cost and without any effect on the environment. These geochemical interpretations are, however, subject to many uncertainties.

Certain chemical reactions between water and wall rock are assumed to take place in the geothermal reservoir deep underground, and the solutes are delivered to the surface in the rising spring waters. The problem is that we cannot be certain of the exact reactions taking place deep underground, and, likewise, we do not know whether other reactions are taking place as the spring waters rise toward the surface. Because of these uncertainties, the accuracy of geochemically estimated underground temperatures cannot be assured unless the estimated temperatures determined by different geochemical methods are in reasonable agreement or unless the temperatures are

verified by other means, such as temperatures measured in a drill hole. The Na-K-Ca method is probably the most reliable of the geochemical methods shown on table 3.

Nevertheless, if general patterns are emphasized and not too much credence given to any single analysis, geochemically predicted source temperatures may be used in making several valuable conclusions with respect to the occurrence of geothermal resources in the Cascade Range. First, all analyzed waters that gave Na-K-Ca temperatures above 100°C, except for the Flaming Geyser (an abandoned coal-test well), are from springs located within 30 km of Mount Baker, Glacier Peak, or Mount Rainier stratovolcanoes. Second, no thermal springs or other waters with Na-K-Ca temperatures exceeding 100°C are associated with Mount St. Helens or Mount Adams stratovolcanoes. Third, out of 17 analyses of water from thermal springs, cold springs, and rivers in Skamania County, none gives a Na-K-Ca temperature over 100°C.

There is considerable variation among calculated Na-K-Ca temperatures for rivers and cold springs, and most Na-K-Ca temperatures are above the actual measured water temperatures. Rather than an indication of a contribution of geothermally heated water to these low-temperature rivers and springs, the somewhat higher than expected Na-K-Ca temperatures probably indicate a failure of the Na-K-Ca geothermometer to express accurately the equilibrium conditions of these waters. The calculated source temperatures yielded by the silica and Na/K geothermometers are also generally higher than should be expected for low-temperature rivers and springs; probably for the same reasons that the Na-K-Ca geothermometer failed to yield reasonable results. Therefore, the chemical data listed for low-temperature waters should probably be used only to indicate that the thermal and some nonthermal waters are chemically anomalous.

TABLE 3.—Chemical data for springs and rivers in the Cascade Range, Washington

Map no.	Name	County	Location ^{1/}	Temperature (°C)	Flow (gpm)	pH	Parts per million						Sampling date	Predicted source temperature (°C) ^{2/}			Source of data ^{3/}	Analysis by ^{4/}
							Cl	Na	K	Ca	SiO ₂	Li		Na-K-Ca ^{5/}	SiO ₂	Na/K		
1	City of Blaine spring	Whatcom	SW $\frac{1}{4}$ 3, (40-1E)	7.3	3.3	5.8	2.0	12	24	4/7/49	22	65	300	1
2	Lorabee Spring	...do...	NW $\frac{1}{4}$ 36, (39-2E)	7.3	22	18	3.0	23	19	4/7/49	42	55	250	1
3	Mount Baker hot spring	...do...	NW $\frac{1}{4}$ SW $\frac{1}{4}$ 20, (38-9E)	42	7	8	108	165	10.0	7.9	140	0.4	162*	157	139	3	UW
do.....do.....do.....	~ 38	6-8	8.3	128	150	13	0.8	10/3/73	173	5	DOE
do.....do.....do.....do.....do.....	7.7	146	158	10	2	~ 1	0.38do.....	142	6	USBM
do.....do.....do.....do.....do.....	8.4	109	154	7.7	16.6	94	0.80do.....	146*	134	124	6	UN
4	U.S. Forest Service spring	...do...	NW $\frac{1}{4}$ 25, (37-8E)	12	7.3	4.0	6.4	2.4	8.4	23	10/27/54	45	64	>300	1
5	Sulphur hot springs	Snohomish	NW $\frac{1}{4}$ 19, (32-13E)	~ 30	1-2	7.8	54	103	1.7	1.0	75	0.2	7/7/62	135*	122	< 80	2	USGS
do.....do.....do.....	37	4	8	52	108	2.4	N.D. ^{6/}	120	0.1	148	< 80	3	UW
do.....do.....do.....	39	2	8.6	100	96	2	< 0.2	0	7/26/71	< 80	4	USBM
do.....do.....do.....	1-2	8.5	55	103	1.4	12	66	0.31	10/3/73	49	114	< 80	6	UN
6	Edwards springs	...do...	SW $\frac{1}{4}$ 24, (31-4E)	10	7.5	3.6	5.6	1.4	9.0	31	9/2/44	29	76	>300	1
7	Kennedy Hot springs ^{7/}	...do...	NE $\frac{1}{4}$ 1, (30-12E)	~ 30	3-5	7.7	643	655	64	37	136	3.3	7/30/61	199*	155	187	2	USGS
do.....do.....do.....	34	7	612	808	67.8	228	380	3.7	177*	227	168	3	UW
do.....do.....do.....	37	4	6.5	676	660	75	73	0	7/26/71	201*	202	4	USBM
do.....do.....do.....	6-8	7.1	28	600	85	125	10/3/73	207*	228	5	DOE
do.....do.....do.....	6-8	7.4	730	688	75	192	~ 0.5	3	10/3/73	190*	197	6	USBM
do.....do.....do.....	6-8	8.4	612	660	71.2	193	167	5.8	10/3/73	189*	167	196	6	UN
8	Upper Kennedy hot spring ^{7/}	...do...do.....	38	4	6.6	681	626	79	69	21	7/26/71	207*	60	213	4	USBM
9	Kennedy No. 3 spring	...do...do.....	~ 21	2-3	8.7	500	562	58.6	157	123	4.7	10/3/73	186*	149	192	6	UN
10	Gamma hot spring	...do...	~ SE. cor. 24, (31-13E)	~ 60	3-4	7.9	728	491	77	47	150	2.6	8/28/62	220*	160	243	2	USGS
11	Garland Mineral Springs ^{8/}	...do...	NW $\frac{1}{4}$ 25, (28-11E)	21	6	2671	1592	130	336	120	7.5	184*	148	167	3	UW
do.....do.....do.....	7	25	6	461	358	27.9	90	N.D.	1.4	167*	162	3	UW
12	Scenic Hot Spring	King	Sec. 28 (26-13E)	10	30	5	N.D.	N.D.	1.2	14	N.D.	N.D.	3	UW
13	Diamond Mineral Spring	...do...	Sec. 21, (21-6E)	11	8	1574	1280	5.5	118	N.D.	N.D.	92*	< 80	3	UW
14	Flaming Geyser well	...do...	SE $\frac{1}{4}$ 27, (21-6E)	12.5	8.5	5600	4640	34.9	54	90	0.4	121*	132	< 80	3	UW
15	Nisqually River	Pierce	SW $\frac{1}{4}$ 34, (15-7E)	8	7.2	2	6.4	4.9	2.3	73	9/6/72	93	120	>300	4	DOE
16	Longmire Springs	...do...	Near SE.cor.29,(15-8E)	21	6	615	402	37.2	298	170	1.8	99	168	180	3	UW
do.....do.....do.....	22	0	7.4	1657	487	41	492	0	2	10/18/73	93	170	6	USBM
17	Ohanapecosh hot springs ^{7/}	Lewis	NW $\frac{1}{4}$ 4, (14-10E)	40	60	7	869	981	50.9	85	80	3.3	164*	125	127	3	UW
do.....do.....do.....	49	3	7.7	915	935	50	64	~ 1.5	3	10/18/73	129	6	USBM
do.....do.....do.....do.....do.....	7.9	867	914	55.3	77	89	4.7	10/18/73	172*	131	138	6	UN
18	Summit Creek Soda Spring ^{7/}	...do...	Near center 18,(14-11E)	13	6	1552	1790	86.7	278	170	5.9	161*	168	122	3	UW
do.....do.....do.....	12	3	7.7	2840	1690	86	257	0	5	10/18/73	163*	126	6	USBM
do.....do.....do.....do.....do.....	7.9	1404	1770	97.6	247	100	7.5	10/18/73	168*	138	132	6	UN
19	Malotte spring	Yakima	SE $\frac{1}{4}$ 32, (16-17E)	17	7.7	1.8	17	4.3	12	53	11/19/48	64	103	>300	1

20	Mulford spring	...	SW $\frac{1}{4}$ 3, (14-18E)	15	...	7.6	9.1	13	5.8	32	66	...	11/19/48	51	114	>300	1
21	Cispus River	Lewis	NE $\frac{1}{4}$ 23, (11-8E)	9	...	7.4	3	4.4	1.3	1.2	28	...	9/6/72	60	72	>300	4	DOE
22	North Fork Toutle River	Cowlitz	SE $\frac{1}{4}$ 33, (10-3E)	11	...	7.5	7	15	1.2	1.5	32	...	9/8/72	66	77	163	4	DOE
23	Clear Creek	Skamania	Sec. 20, (8-7E)	12	...	7.1	4	3.6	0.4	1.7	21	...	9/8/72	22	60	198	4	DOE
24	Lewis River	...	Sec. 25, (8-7E)	10	...	7.2	2	4.2	1.0	1.0	21	...	9/8/72	56	60	>300	4	DOE
25	Landslide spring	...	SW $\frac{1}{4}$ 34, (8-7E)	5.5	...	6.9	<1	3.4	0.2	1.3	9	...	8/30/72	10	<40	137	4	DOE
26	Muddy River	...	NW $\frac{1}{4}$ 1, (7-6E)	9	...	7.4	6	10.3	0.7	1.7	30	...	9/8/72	45	75	145	4	DOE
27	Pine Creek	...	SW $\frac{1}{4}$ 24, (7-6E)	8	...	7.5	7	11.8	1.8	1.1	56	...	9/8/72	82	106	238	4	DOE
28	Spring 72	...	SE $\frac{1}{4}$ 13, (7-7E)	4	...	6.9	1	3.4	0.6	1.0	19	...	8/17/72	40	55	260	4	DOE
29	Lonesome Sale Road spring	...	NW $\frac{1}{4}$ 30, (7-8E)	4.5	...	7.2	6	6.0	0.6	2.0	24	...	8/17/72	33	65	188	4	DOE
30	Spring 710	...	NE $\frac{1}{4}$ 36, (7-7E)	4	...	7.1	1	2.6	0.3	1.5	15	...	8/17/72	15	50	204	4	DOE
31	Bacon Creek spring	Yakima	SE $\frac{1}{4}$ 1, (7-12E)	6	...	6.9	1	59	1.2	0.7	17	...	9/16/72	97	52	<80	4	DOE
32	Gotchen Creek spring	...	SW $\frac{1}{4}$ 18, (7-11E)	3	...	6.9	1	3.4	1.5	0.4	17	...	9/15/72	85	52	>300	4	DOE
33	Trout Lake Creek	Klickitat	NE $\frac{1}{4}$ 8, (6-10E)	12	...	7.4	1	4.4	0.7	1.4	17	...	9/7/72	55	52	244	4	DOE
34	White Salmon River	...	SW $\frac{1}{4}$ 11, (6-10E)	8	...	7.2	2	4.2	1.7	1.3	32	...	9/7/72	66	77	>300	4	DOE
35	White Creek	...	SW $\frac{1}{4}$ 11, (6-13E)	14	...	8.1	15	10.8	1.5	3.3	21	...	9/7/72	54	60	225	4	DOE
36	Bear Creek spring	...	SE $\frac{1}{4}$ 20, (6-10E)	13	...	7.1	1	5.4	0.6	1.7	24	...	8/25/72	35	65	198	4	DOE
37	East Fork Lewis River	Clark	NW $\frac{1}{4}$ 13, (4-3E)	13	...	7.2	5	6.2	0.2	3.3	17	...	9/8/72	2	52	93	4	DOE
38	Iron Mike Spring ^{B/}	Skamania	Sec. 31, (5-7E)	10	...	7	318	211	6.2	192	40	0.4	45	90	89	3	UW
39	Bubbling Mike Spring ^{B/}do.....	8.5	...	6.5	276	176	5.1	154	50	0.3	43	100	88	3	UW
40	Little Iron Mike Spring ^{B/}do.....	10	...	6.5	561	404	9.6	309	N.D.	0.8	55	...	<80	3	UW
41	Little Soda Spring	...	SE $\frac{1}{4}$ 5, (4-7E)	8	...	6	36	28	13.6	46	N.D.	N.D.	77	...	>300	3	UW
42	Wind River	...	NW $\frac{1}{4}$ 15, (4-7E)	13	...	7.2	4	4.0	0.5	1.8	24	...	9/7/72	27	65	212	4	DOE
43	City of Vancouver spring	Clark	SW $\frac{1}{4}$ 33, (2-2E)	10	2.9	4.2	5.6	15	50	...	5/17/49	53	100	>300	1
44	Bonneville hot spring	Skamania	Sec. 16, (2-7E)	32	20	9.5	151	126	1.5	42	N.D.	N.D.	31	...	<80	3	UW
45	St. Martin Hot Springs	...	SE. cor. 21, (3-8E)	49	...	7	636	291	6.2	104	N.D.	0.2	60	...	<80	3	UW
46	Wind River	...	SW $\frac{1}{4}$ 22, (3-8E)	14	...	7.5	4	7.4	0.8	1.7	30	...	9/7/72	45	75	196	4	DOE
47	Little White Salmon River	...	NW $\frac{1}{4}$ 1, (3-9E)	8	...	7.2	2	6.0	1.2	1.3	58	...	9/7/72	59	108	228	4	DOE
48	Leonardo springs	Klickitat	NW $\frac{1}{4}$ 21, (2-13E)	14	5.0	7.8	2.1	22	48	...	7/29/30	27	98	>300	1

^{1/} Locations by legal land description are abbreviated; for example, SW $\frac{1}{4}$ 3, (40-1E) written in full would be southwest quarter of section 3, township 40 north, range 1 east.

^{2/} Na-K-Ca source temperatures were calculated using the formula $\log\left(\frac{Na}{K}\right) + \beta \log\left(\frac{\sqrt{Ca}}{Na}\right) = \frac{1647}{273+t_{oc}} - 2.24$, where Na, K, and Ca concentrations are expressed in molality, β is either 4/3 or 1/3, and t_{oc} is the predicted source temperature in degrees Celsius. A source temperature is calculated using $\beta = 4/3$. If this temperature is greater than 100°C, source temperature is recalculated using $\beta = 1/3$ (Fournier and Truesdell, 1973, 1974).

SiO₂ source temperatures are estimated from curve A of Fournier and Truesdell (1970), which assumes cooling entirely by heat conduction and equilibrium with quartz.

Na/K source temperatures are estimated from curve G of A. J. Ellis (White, 1970).

^{3/} 1 = Van Denburgh and Santos, 1965; 2 = Tabor and Crowder, 1969; 3 = Campbell and others, 1970; 4 = Division of Geology and Earth Resources Files, 1972; 5 = Division of Geology and Earth Resources Files, 1973; 6 = Division of Geology and Earth Resources Files, 1974.

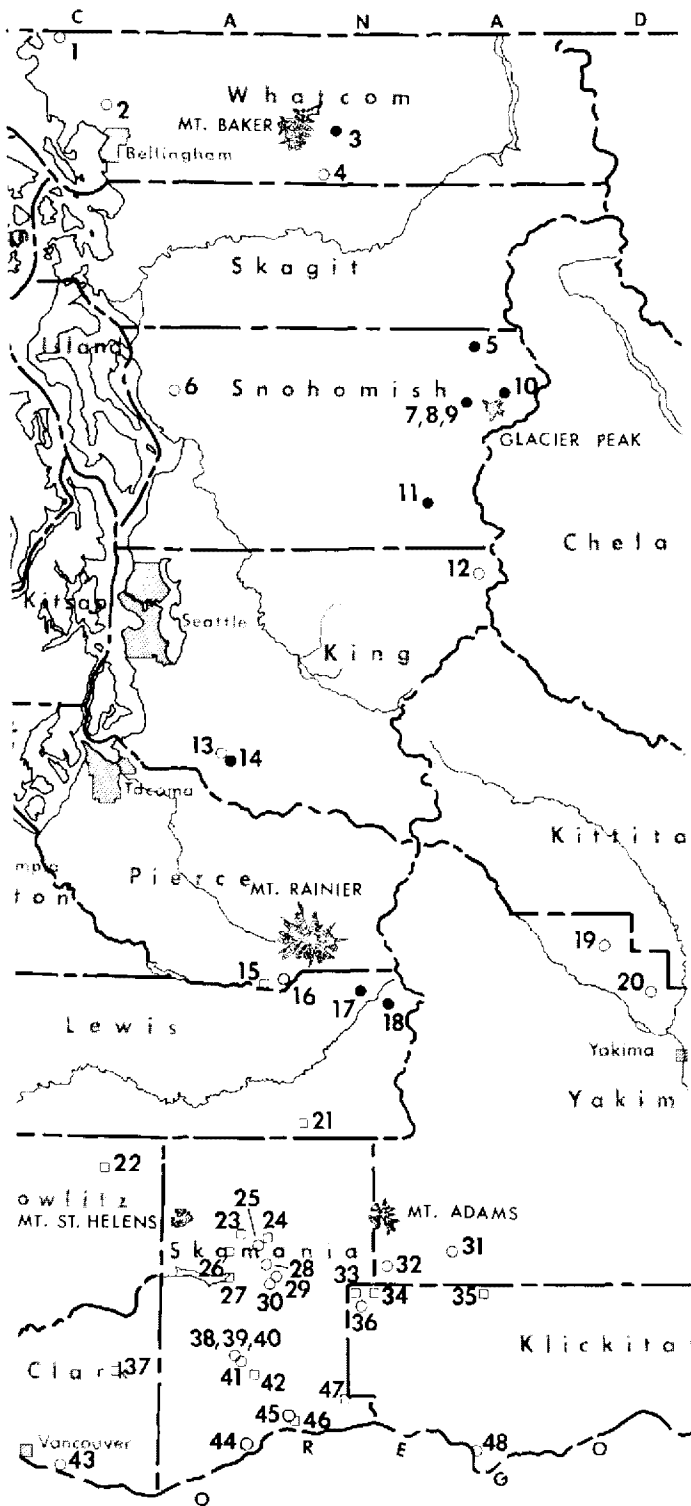
^{4/} UW = University of Washington; DOE = Washington State Department of Ecology; USBM = United States Bureau of Mines, Bartlesville, OK; UN = University of Nevada, Desert Research Institute, Boulder City, NV; USGS = United States Geological Survey.

^{5/} Predicted temperatures marked by an asterisk (*) were calculated using $\beta = 1/3$. Unmarked Na-K-Ca temperatures were calculated using $\beta = 4/3$, see footnote 2.

^{6/} Not detected.

^{7/} Springs with extensive calcareous tufa deposits.

^{8/} Springs known to have precipitates associated with them, but precipitates have not been identified.



- | | |
|-------------------------------|-------------------------------|
| 1. City of Blaine spring | 25. Landslide spring |
| 2. Larabee Spring | 26. Muddy River |
| 3. Mount Baker hot spring | 27. Pine Creek |
| 4. U.S. Forest Service spring | 28. Spring 72 |
| 5. Sulphur hot springs | 29. Lonesome Sale Road spring |
| 6. Edwards springs | 30. Spring 710 |
| 7. Kennedy Hot springs | 31. Bacon Creek spring |
| 8. Upper Kennedy hot spring | 32. Gotchen Creek spring |
| 9. Kennedy No. 3 spring | 33. Trout Lake Creek |
| 10. Gamma hot spring | 34. White Salmon River |
| 11. Garland Mineral Springs | 35. White Creek |
| 12. Scenic Hot Spring | 36. Bear Creek spring |
| 13. Diamond Mineral Spring | 37. East Fork Lewis River |
| 14. Flaming Geyser well | 38. Iron Mike Spring |
| 15. Nisqually River | 39. Bubbling Mike Spring |
| 16. Langmire Springs | 40. Little Iron Mike Spring |
| 17. Ohanapecash hot springs | 41. Little Soda Spring |
| 18. Summit Creek Soda Spring | 42. Wind River |
| 19. Malotte spring | 43. City of Vancouver spring |
| 20. Mulford spring | 44. Bonneville hot spring |
| 21. Cispus River | 45. St. Martin Hot Springs |
| 22. North Fork Toutle River | 46. Wind River |
| 23. Clear Creek | 47. Little White Salmon River |
| 24. Lewis River | 48. Leonardo springs |

See table 3 for chemical data on these waters

- Thermal springs, mineral springs, or cold springs with Na-K-Ca temperatures below 100°C.
- Thermal or mineral springs with Na-K-Ca temperatures above 100°C.
- River water, all with Na-K-Ca temperatures below 100°C.

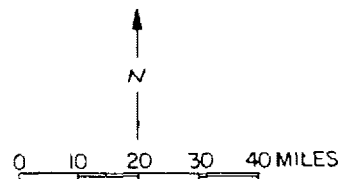


FIGURE 8.—Locations of chemically analyzed springs and rivers in the Cascade Range, Washington.

DRILL HOLES

SITE SELECTION

Geochemical, geological, and some geophysical data, as described earlier in this report, have been gathered in the southern Cascades of Washington during the last several years; but heat-flow determinations have been few because few holes have been drilled in the area. Under sponsorship of the National Science Foundation, the Washington Division of Geology and Earth Resources was able to partially fill this gap during the summer and fall of 1975. Seven heat-flow holes were started in the Indian Heaven area and four of them were drilled to the planned depth of 150 meters. The Indian Heaven area was selected because it is fairly accessible by road while the major stratovolcanoes are not; geologic work by Hammond (1973, 1975) had shown that basaltic volcanism in the area is, at least in part, very young; and gravity studies (Stricklin, 1975) suggested that at least part of the Indian Heaven area was underlain by porous sediments, a zone of fracturing, hydrothermal alteration, or a magma chamber, any combination of which could be taken as favorable for the occurrence of a geothermal reservoir.

The seven holes were sited during a field trip in July 1975. Several factors influenced the selection of sites. We wanted to site all of the holes in the general vicinity of the Indian Heaven fissure zone because we expected that any geothermal heat source in the area would be closely associated with the chain of young volcanoes of the fissure zone. Second, we wanted a uniform distribution of heat-flow holes in order to detect any areal heat-flow gradients that might exist in the area. Third, the prospecting permit issued by the U.S. Forest Service and our drilling budget dictated that drilling be done on or near existing roads. Fourth, we wanted to place at least some

of the holes in Tertiary rocks because we suspected that water circulation in holes drilled into the Quaternary basalts might make it impossible to measure equilibrium temperature gradients. Fifth, the relatively small drilling rigs used were incapable of installing casing through more than about 30 meters of overburden, so we had to site holes in areas of relatively shallow overburden. The selected sites (figs. 1 and 2) are compromises among these factors.

TEMPERATURES

Drill hole DGER 1 was drilled to a depth of only 17.7 m when caving problems forced abandonment of the hole. No temperature-depth measurements were made in this hole. Holes DGER 2, 3, 4, and 5 were completed to a planned depth of 150 m; DGER 6 was drilled to a depth of 80 m (but caved back to 50 m before casing could be installed), and hole DGER 7 was drilled to a depth of 39 m, where cave-in problems caused the drill hole to be abandoned. The temperature results from these various holes will be discussed separately, but the temperature-depth curves for drill holes DGER 2, 3, 4, 5, 6, and 7 are shown together in figure 9 and the average gradients with their standard errors from selected sections of the holes are shown in table 4. The temperature data are tabulated in the appendix. The lithology of the holes is described in table 5 and is briefly discussed in the following section. The relationship of gradient to lithology is discussed in the section on heat flow.

Two sets of temperature data are presented on each of figures 10 through 13: the first type of data is bottom-hole temperature measurements made during drilling; the second type is temperature-gradient measurements made in early October 1975 and September 1976. Soon after the October 1975 logging, snow closed off much of the area for the winter. Since

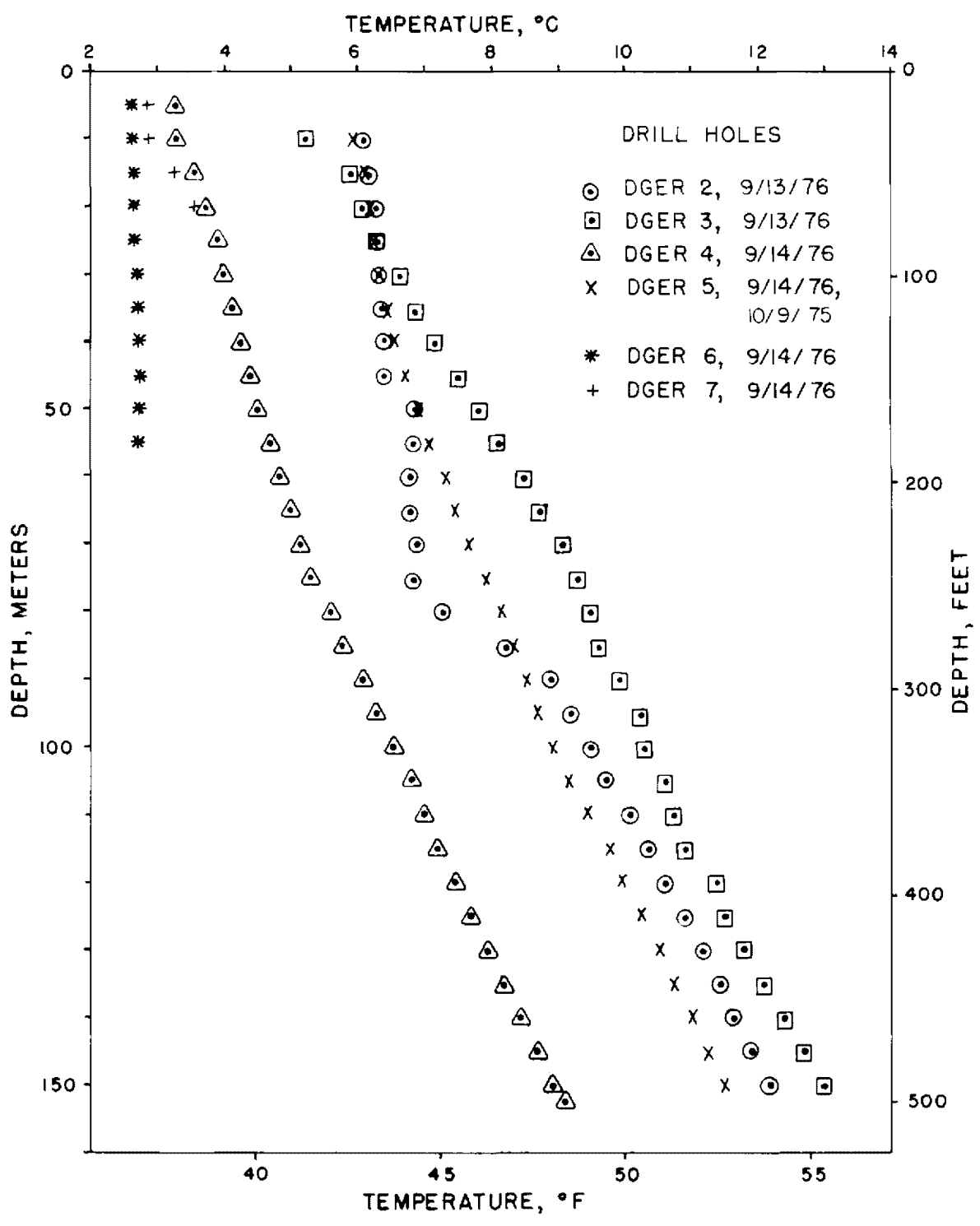


FIGURE 9.—Temperature-depth curves for drill holes DGER 2 through 7.

TABLE 4.—Average temperature gradient, thermal conductivity, and heat-flow measurements for drill holes DGER 2 through 7

Hole no.	North latitude	West longitude	Elevation (meters)	Depth interval (meters)	Thermal conductivity (mcal/cmsec°C)	Number of Samples	Geothermal gradient (°C/km)		Heat flow (mcal/cm ² sec)	
							Uncorrected	Terrain corrected	Uncorrected	Terrain corrected
DGER-2	45°58.6'	121°37.4'	884	100-150	3.40 (0.07) ^{1/}	8	53.8 (0.8)	52.7	1.83 (0.07)	1.79
DGER-3	46°05.9'	121°42.0'	960	40-150	2.96 ^{2/}	4	51.5 (3.0)	46.9	1.52	1.38
				115-150	2.96 (0.27)		58.5 (2.5)	53.4	1.73 (0.18)	1.58
DGER-4	46°07.5'	121°46.2'	1207	15-85	< 4.2	1	30.5 (1.0)		< 1.28	
				85-150	2.99 (0.06)	5	48.5 (0.5)	44.5	1.45 (0.05)	1.33
DGER-5	45°59.9'	121°53.6'	914	100-150	2.94 (0.14)	6	51.0 (0.4)	49.8	1.50 (0.08)	1.46
DGER-6	45°54.8'	121°46.8'	1067	15-55	3.0 ^{2/} (0.5)		2.0		-0.1?	
DGER-7	46°02.9'	121°45.0'	1213	15-25	2.8 ^{2/}		70	58	2.0?	1.6?

^{1/} Values in parentheses are standard errors of the mean.

^{2/} Estimated values.

drilling continued into late September 1975, drilling disturbances were still present in some of the holes during the October 1975 logging. However, these residual disturbances did not preclude accurate gradient determinations as shown by equilibrium temperature data obtained in September 1976.

Terrain corrections were made to the gradients by a technique described by D. D. Blackwell and J. L. Steele. A combined two dimensional-three dimensional technique was used. For the Indian Heaven area, the estimated accuracy of the correction is ± 10 percent of the correction.

BOTTOM-HOLE TEMPERATURE MEASUREMENTS

Because we expected the holes to penetrate relatively permeable and porous volcanic and volcani-clastic rocks, we anticipated that problems might be

encountered involving intrabore circulation between aquifers or between aquifers and the surface because of different piezometric levels in the various fracture zones and aquifers. To some extent this intrabore circulation can be controlled by grouting the hole following completion of drilling; however, if the grout fails to hold, the temperature-depth information from the hole may be permanently lost. Therefore, temperature measurements were routinely made at the bottoms of the holes during drilling. In general, the bottom-hole temperature measurements were made as close as possible to the bottom of the hole before drilling began on the morning shift. Usually a period of 8 to 16 hours had elapsed between the last circulation of drilling fluids and the time of the temperature measurements. Where equilibrium temperatures are known, about half of the bottom-hole measurements are within 0.1°C of the final equilibrium temperatures. The cause of the deviations for the other

TABLE 5.—Thermal conductivity, density, and porosity measurements
for drill holes DGER 2 through 5

Depth (meters)	Density (gm/cm ³)	Porosity (fraction)	K _b ^{1/}	K _{is} ^{2/}
			mcal/cmsec°C	
DGER-2				
102.1	1.87	.30	4.44	3.14
102.1				3.82
107.9	2.03	.24	4.33	3.30
122.2	2.01	.25	5.20	3.75
126.2	1.98	.26	4.27	3.20
137.8	1.91	.29	4.82	3.37
146.0	1.98	.26	4.95	3.56
152.4	1.76	.34	4.98	3.23
DGER-3				
103.6	1.93	.28	3.30	2.60
110.3	2.17	.19		3.18
126.8	2.41	.10	4.27	3.82
129.8	2.00	.25	3.12	2.55
DGER-4				
50.9			4.15	
84.1	1.74	.42	3.0	2.2
104.5	1.87	.30	4.00	2.92
112.2	2.20	.18	3.60	3.04
132.3	1.88	.30	3.97	2.90
141.7	2.18	.18	3.86	3.22
150.9	1.85	.31	3.97	2.88
DGER-5				
56.7			4.97	
88.1			4.79	
105.9	1.99	.26	3.10	2.52
115.5	2.24	.16	3.04	2.69
125.9	2.23	.17		3.08
141.7	2.20	.18	3.74	3.13
153.0	1.85	.31	4.12	2.95
153.0	1.85	.31		3.45

^{1/} Bulk thermal conductivity (for the samples measured by the chip technique).

^{2/} In situ conductivity. The in situ conductivities are either calculated from the porosity and K_b measurements or, if no K_b is shown, determined directly on saturated core samples by the divided bar technique.

temperatures can in most, but not all, instances be explained by drilling and hole conditions at the time of the measurement. If severe hole problems had been encountered so that later temperature measurements could not have been made, the bottom-hole measurements would have provided estimates of the temperature gradients.

The bottom-hole temperature measurement program was a successful aspect of these studies and such measurements are recommended in other similar geologic situations.

TEMPERATURE GRADIENTS

Drill Hole DGER 2

The temperature-depth measurements and bottom-hole temperature data for DGER 2 are shown in figure 10. DGER 2 was drilled to a depth of 153 m and completed September 23, 1975. During the drilling, complete loss of drilling fluid circulation occurred at 68.3 m (this depth is indicated by the arrow on figure 10). The hole was drilled from 68.3 m to 153 m without return of drilling fluid to the surface. Below about 90 m, the temperature depth curve is linear with an average slope of 53.8 ± 0.8 °C/km (all errors shown in this report are standard errors of the mean). Above 90 m, the temperatures depart significantly from a straight line; however, the temperatures measured at 45 m and 50 m are close to the straight-line gradient extrapolated from the 90 m to 150 m interval. Judging from the relationship between the extrapolated gradient and the measured temperatures, it appears that water is moving downward in the well bore between the 50 m and 75 m depths and upward between the 10 m and 45 m depths.

The bottom-hole temperatures measured at 39 m, 50 m, and 67 m are significantly warmer than

the extrapolated equilibrium gradient (the bottom-hole temperature measured at 8 m may be warmer because of seasonal surface-temperature variation). Drilling between 15 m to 68 m was done using re-circulated water which had heated up in the surface holding tanks. Flow of the heated drilling fluid into the lost-circulation zone at or near 68 m probably accounts for the anomalously high bottom-hole temperature measured at 67 m, and significant but undetected drilling fluid loss above 68 m might also account for the anomalous bottom-hole temperatures at 39 m and 50 m.

Drill Hole DGER 3

Drill hole DGER 3 was started on September 10, 1975, and drilling was completed on September 20, 1975, at a depth of 152.4 m. Final grouting of the hole with cement was finished on September 23, 1975. The bottom-hole temperature measurements (fig. 11) at 29 m and 92 m are significantly below the equilibrium temperatures, which is unusual. The geothermal gradients from 115 m to 150 m (58.5 ± 2.5 °C/km), the least disturbed appearing portion of the hole, and from 40 m to 150 m (51.5 ± 3.0 °C/km) are not very different. The drill hole is located on the side of a north-trending valley with a total relief of about 300 m. The terrain correction reduces the gradients for the two intervals to 53.4 and 46.9 °C/km, respectively, because of the valley effect.

Drill Hole DGER 4

A temperature-depth curve and the bottom-hole-temperature measurements for DGER 4 are shown in figure 12. This hole was completed September 9, 1975, at 152.4 m. Upon completion, it was grouted

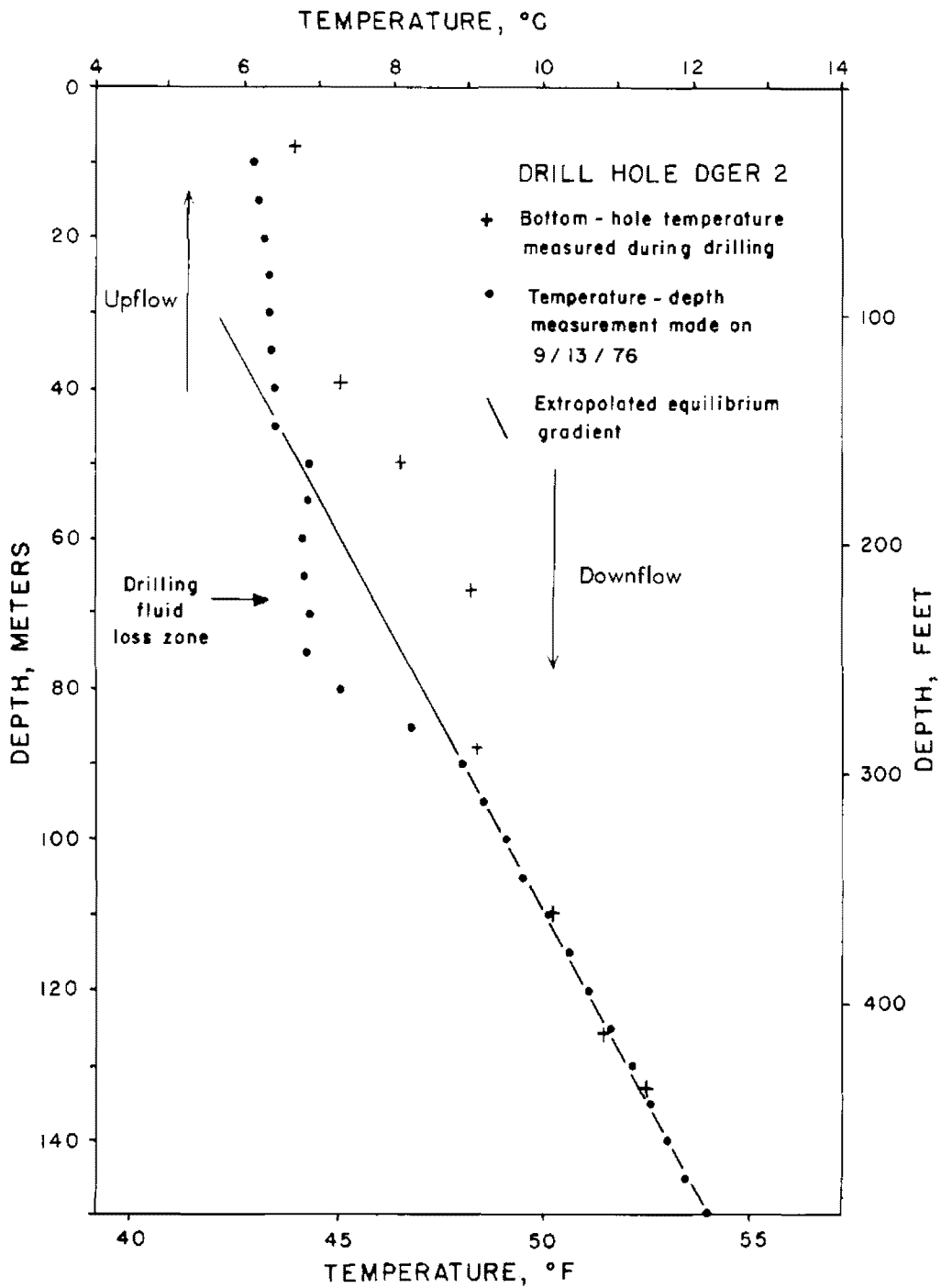


FIGURE 10.—Temperature-depth curve for drill hole DGER 2.

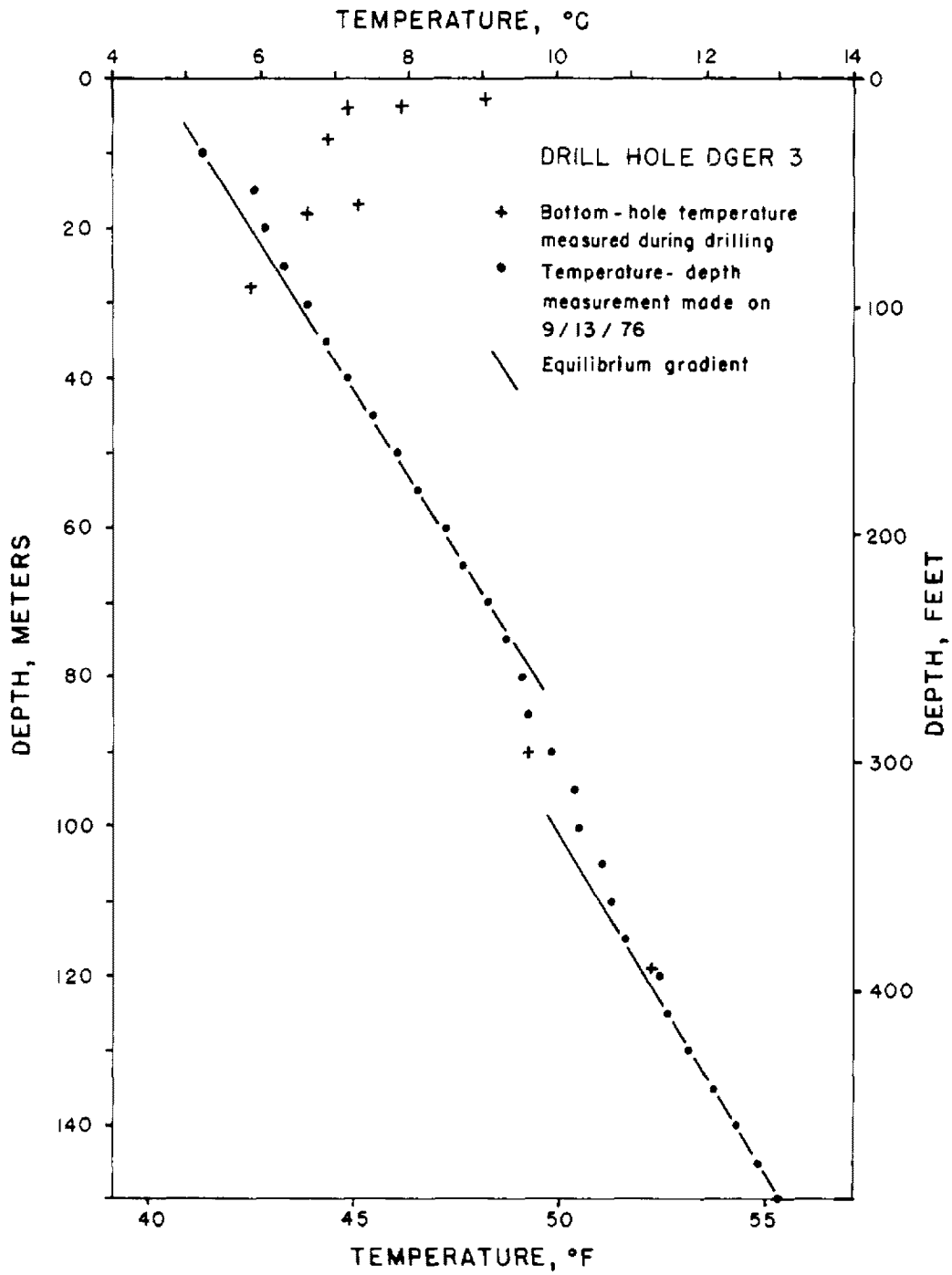


FIGURE 11.—Temperature-depth curve for drill hole DGER 3.

with cement from 108 m to the surface. Extensive drilling-fluid loss occurred in the interval between 55 m and 105 m and a residual drilling disturbance in this fluid-loss zone was still present between 55 m and 75 m during the logging of October 8, 1975. This disturbance had disappeared by September, 1976, as shown by the temperature-depth curve from the final logging (fig. 12). (The magnitude of this drilling disturbance may be ascertained by comparing the temperature-depth logs of October 8, 1975, and September 14, 1976, in the appendix.) The fluid loss may explain the slightly high bottom-hole temperatures measured at 63 m, 91 m, and 103 m. An artesian aquifer was encountered at 108 m and this aquifer was successfully grouted following completion of the drilling. The bottom-hole temperatures at 116 m, 129 m, and 140 m are very close to the temperatures observed after the completion of drilling.

There is a change in the slope of the temperature-depth curve near 85 m which is probably caused by a nearby lithologic change at 80 m. Below the contact the average gradient is $48.5 \pm 0.5^\circ\text{C}/\text{km}$ between 85 m and 150 m. Above 85 m the gradient is significantly lower. The average gradient between 15 m and 85 m is $30.5 \pm 1.0^\circ\text{C}/\text{km}$.

The hole is located on the north side of West Twin Butte, a cinder cone that still preserves most of its original physiographic features and probably is no older than 10,000 years. The terrain correction reduces the gradient by 8 percent.

Drill Hole DGER 5

The temperature-depth curve for hole DGER 5 is shown in figure 13. This curve is smooth with a gradually increasing gradient with increasing depth. The hole is located at the edge of a large clearing

(McClellan Meadows) and the decrease in gradient near the surface is caused by an average surface temperature difference between the clearing, with a relatively higher surface temperature, and the surrounding forest with a lower surface temperature (see Roy, Blackwell, and Decker, 1972). The hole was completed on August 8, 1975, and the temperatures below 50 m were essentially at equilibrium by October 9, 1975.

The low bottom-hole temperatures observed at 93 m, 100 m, and 111 m were caused by artesian flow which was encountered beginning at 58 m. These bottom-hole temperature measurements were made in the early morning from 6 to 17 hours after last circulation of drilling fluids. However, the drill rods were left in the drill hole a short distance from the bottom and the artesian water, in addition to coming straight up the hole, went down to the bottom of the hole and came up through the drill rods, thus lowering the temperatures at the bottom of the hole by this artificial circulation. After this effect was recognized, the rods were removed at least 10 m from the bottom of the hole during the night preceding the bottom-hole measurement at 134 m. The temperatures not affected by the artesian flow (at 35 m, 70 m, and 134 m) agree very closely with the observed equilibrium temperatures.

The best gradient in the hole is $51.0 \pm 0.4^\circ\text{C}/\text{km}$ in the interval from 100 m to 150 m. The topographic correction decreases the gradient to $49.8^\circ\text{C}/\text{km}$. No correction has been made for the clearing effect present above 100 m.

Drill Hole DGER 6

Temperature-depth measurements from DGER 6 are shown in figure 9. This hole was originally drilled

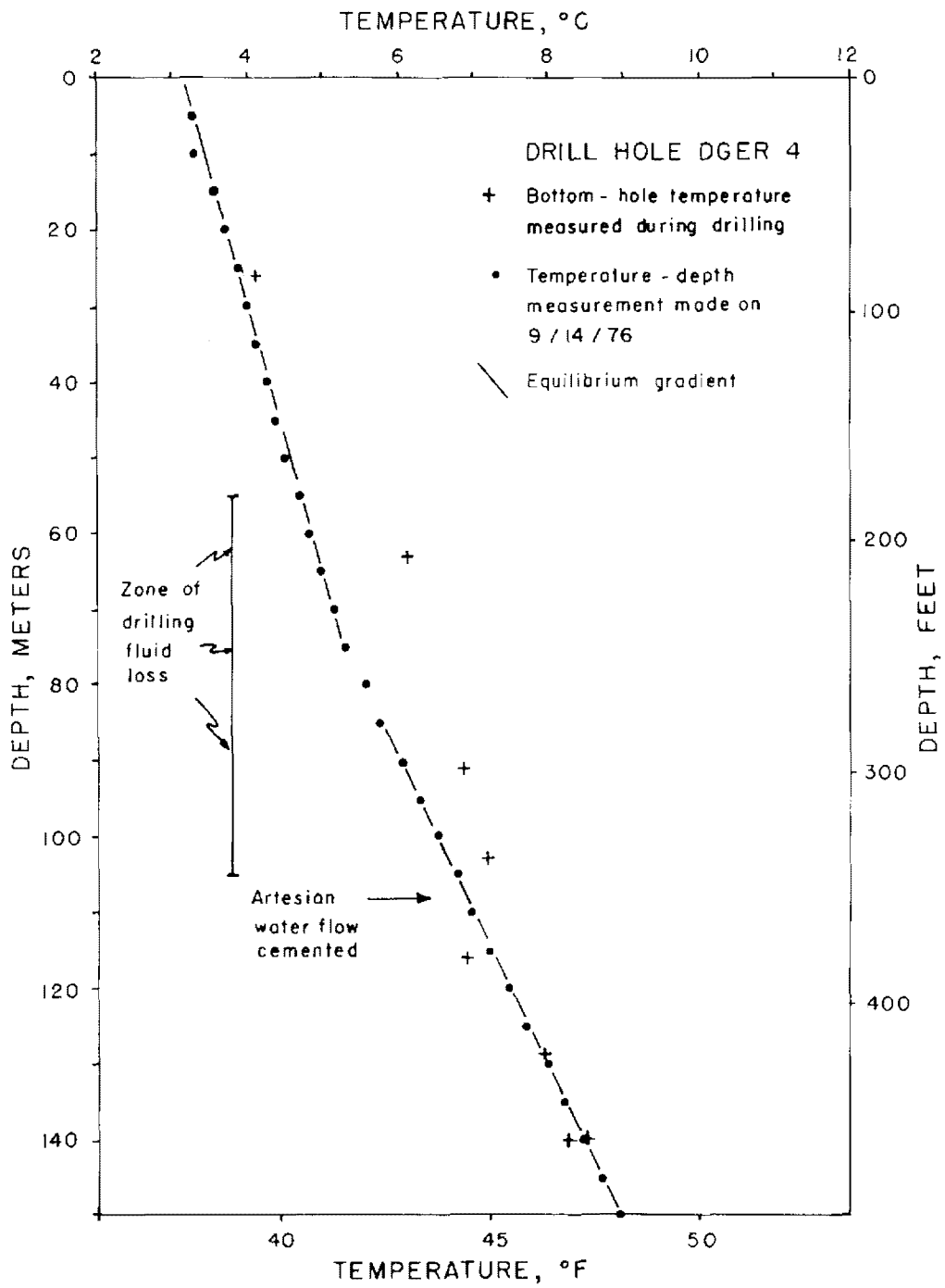


FIGURE 12.—Temperature-depth curve for drill hole DGER 4.

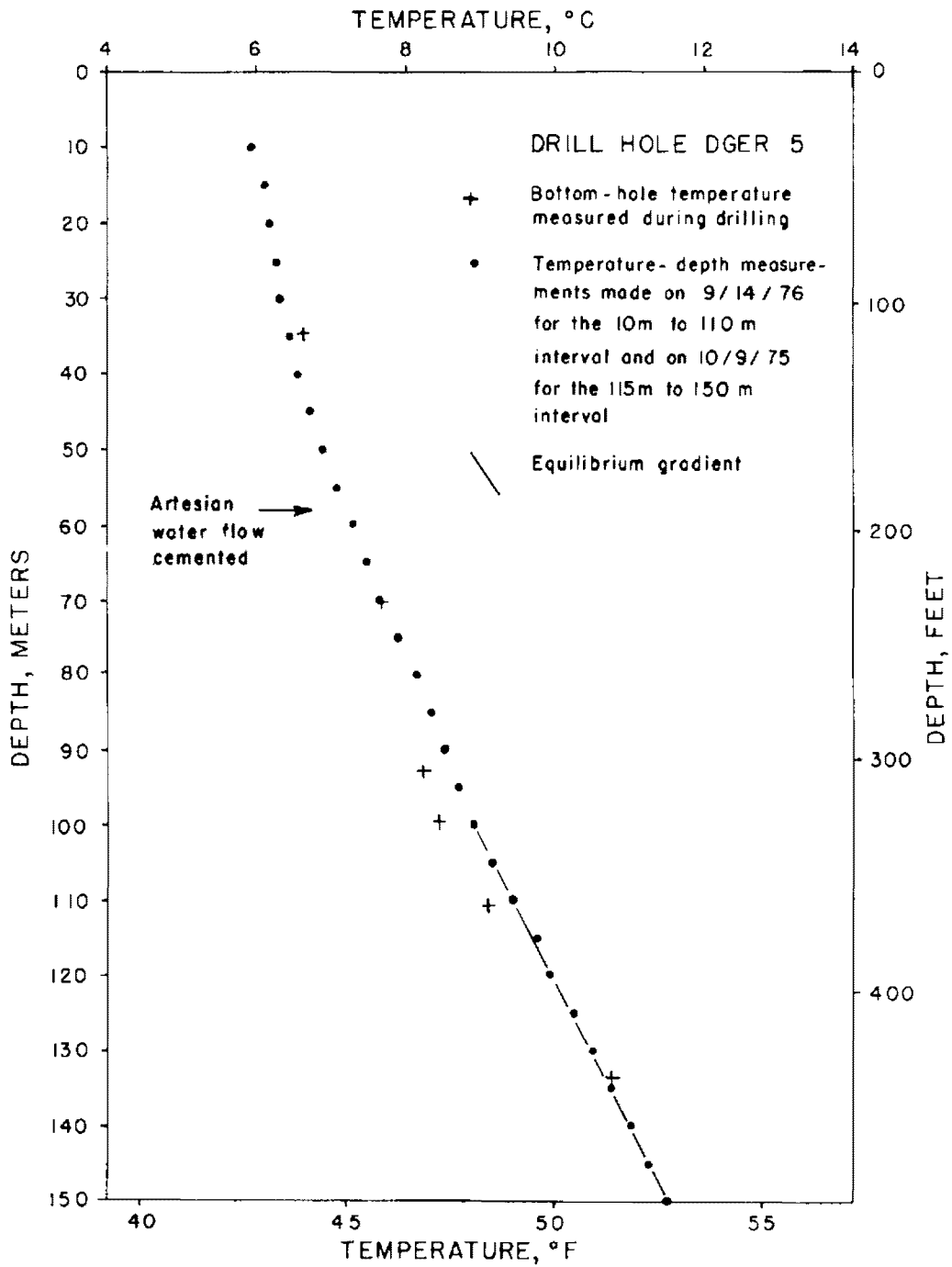


FIGURE 13.—Temperature-depth curve for drill hole DGER 5.

to a total depth of 83.5 m, however, the drill bit was stuck in the hole and the hole had to be abandoned. During casing of the hole a cave zone prevented insertion of the pipe below 56 m. The temperature-depth curve is highly irregular and suggests that there is no temperature increase with depth, in fact there may even be a slight decrease. The bottom-hole temperatures also suggest no temperature increase with depth. This hole was drilled entirely in Quaternary basalts at the edge of the Big Lava Bed. The hole is above the water table, which elsewhere is at shallow depths, and the temperature appears to be decreasing slightly with depth. It appears that water is entering the permeable lava flows and flowing through the lava toward lower elevations. In this area the lava flows followed valleys extending all the way to the Columbia River. Perhaps these buried river valleys are serving as channels for flow of ground water down toward the Columbia.

The near-zero gradient in this hole is probably characteristic of the rock around it and another hole nearby would likely observe the same temperatures. In this case the water disturbance is of a regional nature rather than confined to the bore hole as is the case in drill hole DGER 2 (fig. 10). Although this conclusion is clear given the whole set of data, if only the upper 70 m of DGER 2 had been logged the two types of disturbance might have been confused and incorrectly interpreted. The original bottom-hole temperature measurements in DGER 2 illustrate the difference in the undisturbed, equilibrium gradient between it and DGER 6.

Drill Hole DGER 7

DGER 7 was drilled in a valley (Cultus Creek) heading near the axis of the Indian Heaven fissure

zone. The drill hole started out in unconsolidated glacial outwash or till material and penetrated a lava flow in the lower part of the hole. The unconsolidated sediments did not permit completion of the hole to the projected depth, the hole was abandoned at 39 m, and 29 m of 2.5 cm iron pipe was installed in the hole. There is a gradient in the hole of 70°C/km between 15 m and 25 m (fig. 9). The terrain correction is relatively large because the hole is in a rather deep valley. The terrain corrected value is 58°C/km, a lower limit for the gradient at this site.

THERMAL CONDUCTIVITY

DETERMINATIONS

Thermal conductivity measurements were made on samples from the four deep drill holes in order to obtain data for calculation of heat flow values. The details of the thermal conductivity measurements as well as some density and porosity calculations on the samples are shown in table 5, and lithologies are presented in table 6. Thermal conductivity measurements were made using two different techniques. The first is a conventional divided-bar technique similar to that described by Birch (1950) and Roy, Blackwell, and Birch (1968). Measurements were made on water-saturated samples in order to match the in situ conditions. This technique is the most precise and accurate of all conductivity measurement techniques and has an estimated precision of ± 1 percent and an accuracy of ± 5 percent. Because of the general high porosity and friable nature of the samples, it was very difficult to make adequate cylindrical samples for the divided bar technique, and many of the samples disintegrated when attempts were made to saw, polish, and resaturate them after they had dried out during shipping.

34 HEAT FLOW STUDIES

The needle-probe technique could not be used because of the coarse-grained nature of many of the rocks (volcaniclastics). Most of the thermal conductivity measurements, therefore, were made on crushed core samples by the divided-bar chip technique described by Sass and others (1971). This technique is not quite as accurate as the solid-sample divided-bar technique because corrections must be made for the porosity of the sample. The estimated precision of the technique is about ± 5 percent and the accuracy is ± 10 percent. The thermal conductivity values for samples that were run with the divided-bar technique and with the chip-sample technique agree closely for this set of data. The technique used for each sample is indicated in table 5. The numbers of samples, and average thermal conductivities for samples from the six drill holes are listed in table 4 and are described briefly below.

Drill hole DGER 2 was drilled to a total depth of 153 m in the Eocene-Oligocene Ohanapecosh Formation. This formation as cut by the drill hole is composed of light- to dark-green volcaniclastic rocks with considerable green clay. The thermal conductivity values measured for samples from this formation are somewhat higher than for the remainder of the formations in the area and it appears that the rocks, cut by this particular hole at least, might have a slightly higher silica content than the rocks cut in the remainder of the drill holes.

Drill hole DGER 3 was drilled to a total depth of 153 m in interlayered volcaniclastic rocks. The formation cut by the drill hole is the Ohanapecosh.

Drill hole DGER 4 was drilled at the foot of a cinder cone (West Twin Butte) and penetrated slightly over 75 m of vesicular basalt flows (basalts of Mosquito Lake). Then 30 m of siltstone, one meter of basalt, and interbedded basaltic siltstones and sandstones of the Eagle Creek Formation? were drilled

to the total depth of the hole at 152.4 m. A basalt sill at 107 m may be an intrusive equivalent of the Quaternary basalts. There is an apparent change in slope of the temperature-depth curve (fig. 12) for DGER 4 near 85 m. This depth corresponds approximately to the lithologic contact between the vesicular basalt and the Eagle Creek Formation?. Heat flow should be the same above and below the contact, but measurements of thermal conductivity do not document a change in thermal conductivity as great as the change in gradients (table 4), in fact the thermal conductivity values are almost the same (table 5). The average fractional porosity for the sedimentary rock in DGER 4 is about .25, and thus the average in situ thermal conductivity value is 2.99 mcal/cmsec°C for all of the samples below 85 m. The maximum thermal conductivity contrast that can be expected would occur if the basalt has zero porosity. This contrast in porosity would lead to a thermal conductivity contrast of about 30 percent, almost enough to explain the change in gradient. Since the average porosity of the basalt section is not known, the exact thermal conductivity for the basalt cannot be obtained, but there is probably not a sufficient thermal conductivity contrast to yield the same heat-flow value for the two sections of the drill hole and explain the observed contrast in geothermal gradients.

Drill hole DGER 5 was drilled to 152 m in vesicular to dense basalt of the Miocene pre-Eagle Creek volcanic and sedimentary rocks. At 102 m the drill hole passed into volcanic sandstone and conglomerate, still part of the pre-Eagle Creek volcanic and sedimentary rocks. The thermal conductivity values for the basalt again depend in detail on the average porosity, which is not well known because of the difficulty of coring interbeds and tops and bottoms of flows. There is a systematic increase in gradient with

depth in DGER 5, but this gradient change is due to proximity to a clearing (McClellan Meadows) and not due to thermal conductivity changes.

No measurements were made of thermal conductivity values on samples from DGER 6. The hole was drilled to a depth of 83.5 m in Quaternary basalts. The section cut by the hole included numerous very thin flows of vesicular to scoriaceous basalt. Although no measurements were made of thermal conductivity in this hole, based on the thermal conductivity values in the basalts from the other holes, it is estimated that the thermal conductivity in the hole is 3.0 ± 0.5 mcal/cmsec°C. The exact determination of the conductivity is not important in view of the negative temperature gradient observed in this hole.

Drill hole DGER 7 had to be terminated at a depth of only 39 m. Little core was recovered from the upper portion of the hole and thus the lithologic section is not well known. It appears to be primarily glacial drift or till. In view of all the uncertainties the exact thermal conductivity for this hole is not critical. The thermal conductivity value was estimated by averaging all of the Quaternary basalt bulk thermal conductivity values (4.5 mcal/cmsec°C), assuming a porosity for these unconsolidated glacial sediments of 0.4, and calculating an in situ thermal conductivity of 2.8 mcal/cmsec°C. The estimated uncertainty of this value is 10-20 percent.

The average thermal conductivity values in the different holes and in the different units in the area are very similar, with the range of thermal conductivity values in the holes penetrating to bedrock being about 2.9 to 3.4 mcal/cmsec°C. Typical porosity values for the units are 0.2-0.3 and typical densities for the pre-Quaternary units are 1.9-2.3 gm/cm³.

HEAT FLOW

Heat-flow values have been calculated for all six drill holes, but different reliabilities are assigned to the heat-flow values from the various holes. The heat-flow values are the mathematical product of the mean harmonic thermal conductivity (table 4, column 6) and the slope of a least-squares straight-line fit to the measured temperature gradient in the depth interval indicated. The calculated error of the heat flow is statistical and relates only to the internal consistency of the data. The actual error estimates of the heat-flow values will be discussed briefly at the end of this section. The heat-flow values are listed in table 4 and the terrain-corrected values are shown in figure 14. A terrain-correction technique developed by D. D. Blackwell and J. L. Steele was used.

Heat flow was calculated for the depth interval 100 m to 150 m for DGER 2. Above 100 m there is an intrabore water-flow disturbance which destroys the in situ gradient. The uncorrected heat flow is $1.83 \mu\text{cal/cm}^2\text{sec}$ and the terrain corrected heat flow is $1.79 \mu\text{cal/cm}^2\text{sec}$.

Heat-flow values calculated for two intervals in DGER 3 (40 m to 150 m and 115 m to 150 m) differ by $0.20 \mu\text{cal/cm}^2\text{sec}$. The terrain correction decreases the heat flow by about 10 percent. The temperature-depth curve (fig. 11) shows several distinct segments with different gradients (for example 25 m to 70 m, 70 m to 115 m, and 115 m to 150 m) that might be related to lithologic changes. However, no thermal conductivity measurements were made above 104 m, and no lithologic differences were noted when cores and cuttings were examined. Thus the best value is the terrain-corrected heat flow be-

TABLE 6.—Lithology of heat-flow drill-holes, Steamboat Mountain-Lemei Rock area,
Skamania County, Washington

Drill hole number	Depth interval (meters)	Lithology	Name
DGER 1	0 to 12.5	Basalt, black, closely jointed	Basalt of the Columbia River Group Ohanapecosh Formation (weathered) or interbed in Columbia River Basalt
	12.5 to 17.7	Sand, medium-grained, unconsolidated	
DGER 2	0 to 47.5	Tuff, ash-flow	Ohanapecosh Formation, 0 to 152.7 m
	47.5 to 48.5	Sandstone, volcanic, with carbonaceous fragments	
	48.5 to 74.1	Lahars (mudflow breccias and conglomerates)	
	74.1 to 75.9	Sandstone, volcanic	
	75.9 to 76.5	Lahar	
	76.5 to 106.5	Tuff, ash-flow	
	106.5 to 129.5	Lahars	
	129.5 to 152.7	Sandstone, volcanic, fine- to coarse-grained	
DGER 3	0 to 12.2	Drift, glacial	Ohanapecosh Formation, 12.2 to 129.8 m
	12.2 to 28.8	Mudstone, siltstone, and fine- to medium-grained sandstone. All of volcanic origin and all containing carbonaceous material	
	28.8 to 29.0	Sandstone, arkosic, coaly	
	29.0 to 54.9	Mudstone and fine-grained sandstone, all of volcanic origin	
	54.9 to 60.0	Lahars, angular clasts	
	60.0 to 75.6	No core recovery	
	75.6 to 78.0	Lahars, angular clasts	
	78.0 to 88.7	No core recovery	
	88.7 to 90.2	Siltstone and medium-grained basaltic sandstone	
	90.2 to 103.0	No core recovery	
	103.0 to 104.5	Siltstone, carbonaceous, with thin coal beds	
	104.5 to 111.6	Lahars, rounded clasts up to 10 cm in diameter and smaller angular clasts	
	111.6 to 126.8	No core recovery	
	126.8 to 129.8	Lahars, angular clasts up to 1 cm in diameter	
	129.8 to 152.4	No core recovery	

Continued

TABLE 6.—Lithology of heat-flow drill-holes, Steamboat Mountain-Lemei Rock area,
Skamania County, Washington—Continued

Drill hole number	Depth interval (meters)	Lithology	Name
DGER 4	0 to 3.7	Cinders	Cinders of West Twin Butte, 0 to 3.7 m
	3.7 to 79.2	Basalt, dense to scoriaceous, up to 20 percent olivine; probably several flows. Rock in lower part of interval is often glassy, broken, and palagonitic	Mosquito Lake basalt, 3.7 to 79.2 m
	79.2 to 89.9	Siltstone and interbedded fine-grained basaltic sandstone. There may be two thin basalt flows in this interval	Eagle Creek Formation?, 79.2 to 107.3 m
	89.9 to 107.3	Mudstone, siltstone, and fine- to coarse-grained sandstone	
	107.3 to 108.4	Basalt, sill	Correlation unknown
	108.4 to 119.2	Mudstone, siltstone, and fine- to coarse-grained sandstone	Eagle Creek Formation?, 108.4 to 152.4 m
	119.2 to 121.0	Grit, basaltic, with clasts up to 1.5 cm in diameter at bottom of interval	
	121.0 to 123.2	Mudstone and siltstone with fine-grained carbonaceous material and irregular masses of carbonized wood	
	123.2 to 127.6	Sandstone, basaltic, very coarse, grades downward to basalt pebble and boulder conglomerate	
	127.6 to 133.2	Mudstone, carbonaceous, grades downward to interbedded mudstone and coarse-grained sandstone with mudstone clasts up to 2 cm in diameter	
	133.2 to 143.6	Mudstone, siltstone, and coarse- to very coarse-grained sandstone, interbedded, scattered pebbles of basalt toward bottom of interval	
	143.6 to 146.3	Conglomerate, with pebbles up to 4 cm in diameter of a porphyritic igneous rock, grades downward to coarse- and fine-grained sandstone to siltstone and mudstone at bottom of interval	
	146.3 to 152.4	Mudstone, siltstone, fine- to coarse-grained sandstone, and conglomerate with well-rounded pebbles of intrusive igneous rock. Interbedded	

Continued

TABLE 6. —Lithology of heat-flow drill-holes, Steamboat Mountain-Lemei Rock area,
Skamania County, Washington—Continued

Drill hole number	Depth interval (meters)	Lithology	Name
DGER 5	0.3 to 75.0	Basalt, fine- to coarse grained, black to brick-red, nonvesicular to very vesicular. Ten percent olivine	Pre-Eagle Creek volcanic and sedimentary rocks 0.3 to 152.4 m
	75.0 to 75.6	Sand, silt, and basalt fragments. Interflow zone	
	75.6 to 101.5	Basalt, red, gray, and black, dense to scoriaceous, 10 percent olivine	
	101.5 to 101.8	No core recovery	
	101.8 to 108.2	Conglomerate, tan to dark-green clasts are rounded to angular, up to 3 cm in diameter, and composed of volcanic rocks	
	108.2 to 108.8	Siltstone, light greenish-gray	
	108.8 to 110.9	Sandstone and siltstone with scattered clasts up to 2 cm in diameter. Clasts are volcanic rock	
	110.9 to 116.4	Conglomerate, clasts are volcanic rock	
	116.4 to 118.0	Siltstone with scattered clasts of altered volcanic rock	
	118.0 to 124.4	Breccia, volcanic rock clasts	
	124.4 to 126.5	Conglomerate with clasts up to 6 cm in diameter of porphyritic volcanic rocks	
126.5 to 152.4	Lahar. Contains both angular and rounded clasts of volcanic rock. Angular clasts are mostly 1 cm or less in diameter. Rounded clasts are up to 4 cm in diameter and are porphyritic volcanic rock		
DGER 6	0 to 1.2	Soil	Cinders of South Red Mountain, 1.2 to 4.0 m Papoose Mountain basalt, 4.0 to 60.0 m Black Creek basalt, 60.0 to 83.5 m
	1.2 to 4.0	Cinders	
	4.0 to 60.0	Basalt, gray to black to brick-red, slightly vesicular to scoriaceous, 20 percent olivine, probably many flows	
	60.0	Basalt, black to red, dense to scoriaceous, 10 to 15 percent olivine. Probably several flows	
DGER 7	0 to 32.9	Drift, glacial	Little Deer Point basalt, 32.9 to 38.7 m
	32.9 to 38.7	Basalt, gray to reddish-gray, slightly vesicular to scoriaceous, 10 percent olivine. Probably two flows	

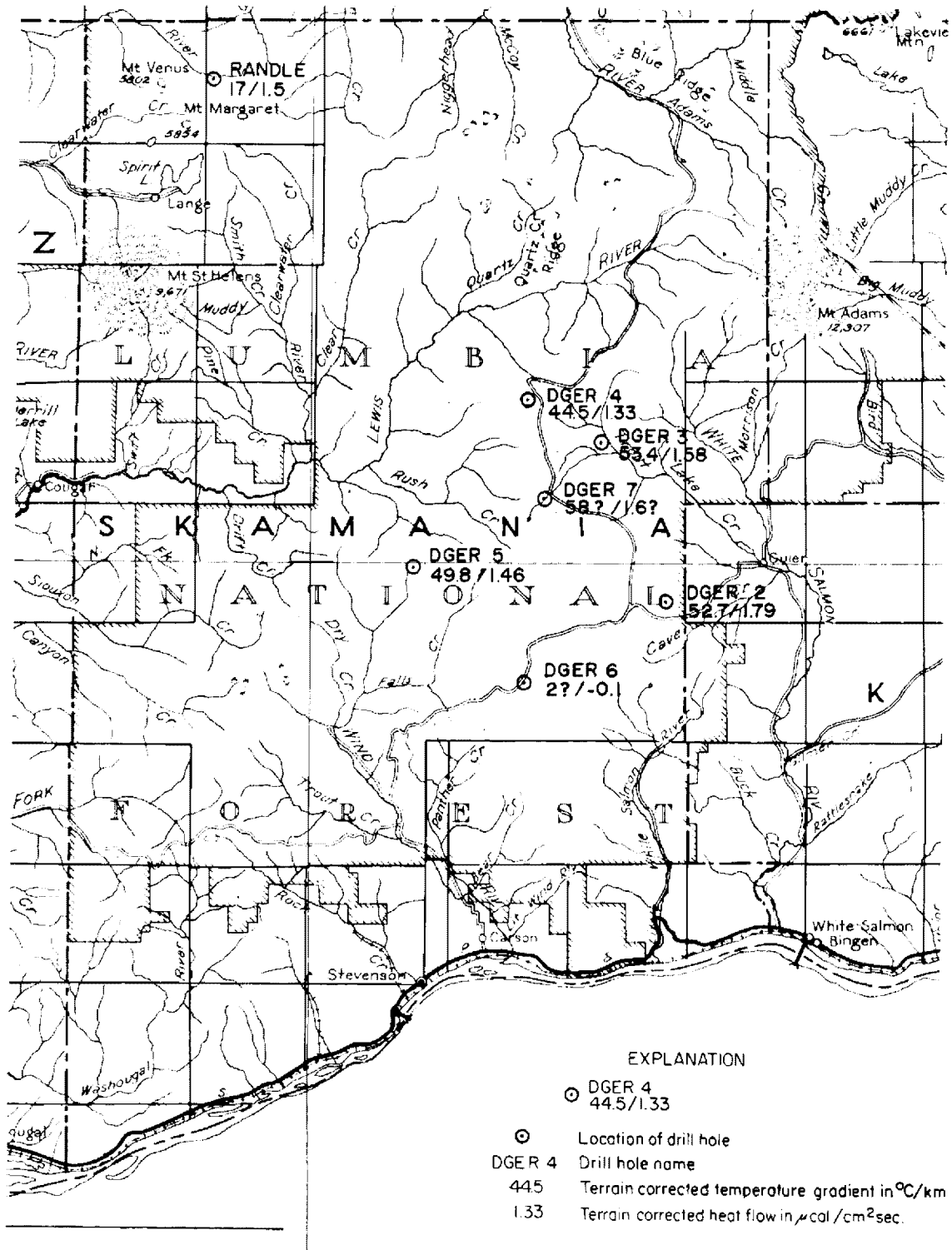


FIGURE 14.—Heat-flow map for the Indian Heaven area, Skamania County, Washington.

tween 115 m and 150 m, where thermal conductivities were measured.

The heat flow was calculated for two intervals in drill hole DGER 4 (15 m to 85 m and 85 m to 150 m). The maximum heat flow in the 15 m to 85 m interval is about $1.3 \mu\text{cal}/\text{cm}^2\text{sec}$. There is a large swamp and a clearing within 50 m from the collar of the drill hole and these surface conditions might explain the low heat flow observed in the upper part of the drill hole. However, the gradient and heat flow seem to change abruptly at a depth which corresponds approximately to the lithologic boundary between the Quaternary lavas and the underlying Eagle Creek Formation?. The terrain-corrected heat-flow value for the 85 m to 150 m interval ($1.33 \mu\text{cal}/\text{cm}^2\text{sec}$) is considered the most reliable. This value might be 5-10 percent low due to the nearby clearing and lake, but surface temperatures are not known well enough to make a correction.

Drill hole DGER 5 intersected two lithologies. It is difficult to estimate the average in situ porosity of the lava flows of pre-Eagle Creek volcanic and sedimentary rocks in order to calculate a heat-flow value. There is no significant change in the temperature gradient that corresponds to the lithologic boundary. The slightly increasing gradient with increasing depth is correlated with the proximity to a large clearing (McClellan Meadows). The best value of heat flow is taken to be the interval between 100 m and 150 m. The terrain-corrected heat flow in this interval is $1.46 \mu\text{cal}/\text{cm}^2\text{sec}$ (the terrain correction is very small).

As illustrated in figure 9 the average gradient in DGER 6 is negative. Combined with the estimated thermal conductivity value (table 4) the resulting heat flow is $-0.1 \mu\text{cal}/\text{cm}^2\text{sec}$. Obviously this heat flow does not reflect the heat flow from the interior

of the earth and the implications of this value will be presented in the discussion section. The value is calculated here merely for reference purposes and is not intended to be taken as a regionally significant heat-flow value.

Drill hole DGER 7 is very shallow and no core samples were available, however, the estimated thermal conductivity is probably within ± 20 percent of the in situ conductivity. The terrain correction is rather large because the drill hole is in a sizeable valley. The best heat-flow value is $1.6 \mu\text{cal}/\text{cm}^2\text{sec}$. In view of the shallow depth of the hole the heat-flow value has a high possible error.

In all the holes, the heat-flow values from the deepest intervals are considered the most reliable. The upper parts of some of the holes show the effects of lateral surface temperature variations for which corrections have not been made. For the bottom intervals of the holes, the terrain-corrected heat-flow values are 1.8, 1.6, 1.3, and $1.5 \mu\text{cal}/\text{cm}^2\text{sec}$ for DGER 2, 3, 4, and 5, respectively. Estimated heat flow values for DGER 6 and 7 are -0.1 and $1.6 \mu\text{cal}/\text{cm}^2\text{sec}$, respectively. The estimated precision of the four values in holes that were drilled to 150 m is ± 5 -10 percent. Values from DGER 6 and 7 are estimates only and subject to very large error. In particular, the value from DGER 6 certainly does not represent the regional heat flow in the Indian Heaven area.

DISCUSSION

The three values of heat flow around the margins of the Indian Heaven basalt field range from 1.5 to $1.8 \mu\text{cal}/\text{cm}^2\text{sec}$ (DGER 2, 3, and 5) and thus span a difference of less than 20 percent. The average

heat flow is $1.6 \pm 0.2 \mu\text{cal}/\text{cm}^2\text{sec}$. One deep hole in the Indian Heaven fissure zone (DGER 4) has a slightly lower heat-flow value of $1.3 \mu\text{cal}/\text{cm}^2\text{sec}$. On the basis of these heat-flow data, we can infer that there is no major geothermal anomaly associated with Indian Heaven fissure zone, and the heat-flow values in the Indian Heaven area do not appear to be significantly affected by water circulation except at DGER 6 at the southern end of the fissure zone.

The regional heat flow of the Cascade Range is not well known. The available determinations range from a high to $1.7 \mu\text{cal}/\text{cm}^2\text{sec}$ near the Canadian border at Mazama, along the eastern margin of the province, to $1.2 \mu\text{cal}/\text{cm}^2\text{sec}$ near Snoqualmie Pass (Blackwell, 1974). The heat-flow value nearest to the Indian Heaven area is south of Randle, approximately 50 km to the northwest (Blackwell, 1974). This value is $1.5 \mu\text{cal}/\text{cm}^2\text{sec}$. The reliable heat-flow values in the Indian Heaven area (ranging from 1.3 to $1.8 \mu\text{cal}/\text{cm}^2\text{sec}$) are compatible with the heat-flow values observed near Randle and Mazama. The Snoqualmie Pass determination is closer to the west margin of the Cascade Range than any of the other data and this geographic difference may explain the difference in heat flow.

Because of the uncertainty of the type of basement rock in the area it is impossible to estimate the average radioactivity of the crust. No measurements of the radioactivity of the Ohanapecoh Formation have been made; however, based on its lithology, the heat production should be between 1 and $3 \times 10^{-13} \text{cal}/\text{cm}^3\text{sec}$. If the mantle heat flow in the Cascades is $1.4 \mu\text{cal}/\text{cm}^2\text{sec}$, which is typical of many of the thermally anomalous regions in the western United States (Roy and others, 1968; Blackwell, 1971, 1973; Roy and others, 1972), then predicted values of surface heat flow would range from 1.5 to $1.7 \mu\text{cal}/$

cm^2sec . Therefore, it appears that the values measured in the Indian Heaven area are what would be expected to be typical regional heat-flow values for the Cascade Range.

The fact that the values are about 10 percent higher along the east edge of the Indian Heaven basalt field (toward the Quaternary andesite volcano of Mount Adams) may not be significant. Because the lateral resolution of buried heat sources with heat-flow measurements is not great (see Blackwell and Baag, 1973; Lachenbruch and others, 1976). The data of this report have little or nothing to say about possible magma chambers beneath Mount Adams or Mount St. Helens, and no heat-flow measurements have been made in the vicinity of either mountain. The $1.8 \mu\text{cal}/\text{cm}^2\text{sec}$ heat-flow value is the closest value to Mann Butte, a possible Quaternary silicic plug located about 6 km away, but this relationship is of doubtful significance. It is clear that there is no large-sized heat source body within the general area of the heat flow study; however, small heat sources could exist in the area and remain undetected because of the relatively wide spacing of our heat-flow measurements.

The general structure of the Indian Heaven fissure zone is a carapace of lava flows extending downward in elevation toward the east and west from an axis along the fissure zone. Because of the high rainfall of the area (over 150 cm per year) and the porous nature of the basalts, it was anticipated that problems with ground-water flow might affect interpretation of the heat-flow data. In view of the agreement of values observed it seems that this circulation is only a local problem. The low heat-flow value which is observed in the shallow part of DGER 4 might be related to ground-water flow, however, it also might be related to the presence of a surface

temperature anomaly associated with Mosquito Lake. It is impossible to resolve this uncertainty without a more complete analysis of the possible effect of the clearing about Mosquito Lake than was done here.

There is definite water flow in the vicinity of DGER 6. The Quaternary lava field extends east along Trout Lake valley and to the south along Lava Creek filling these preexisting valleys (see fig. 1). The lava flows follow the valleys for up to 20 km toward the Columbia River. It may be that these valleys were deeply incised when the lavas were extruded and, consequently, there is a thick fill of lava in the valleys, and the lavas act as conduits for subsurface water circulation toward the Columbia River. If so, the circulation appears to be confined to these preexisting stream valleys and does not include the main portion of the Indian Heaven area. The lava flows extend in the wrong direction to have the water circulation in lava flows directly recharging a ground water system connected to the hot springs, which occur to the southwest along the Columbia River (see fig. 8). It may be that water infiltrates along the Indian Heaven fissure zone and makes its way into a ground water system that feeds the hot springs, but the geologic structure between the Indian Heaven area and the hot springs is quite complex, and this appears to be unlikely.

The average gradient observed in the Indian Heaven area is about $50^{\circ}\text{C}/\text{km}$, and, assuming that this gradient is present in the vicinity of St. Martin's Hot Spring, subsurface circulation of water to a depth of only 1 km would heat the water to the 50°C temperature observed at St. Martin's, which is the warmest spring in the area. The geochemical information from other thermal and mineral springs in the area fails to suggest subsurface heating above 100°C , and, in fact, those predicted temperatures that differ sig-

nificantly from measured water temperatures may do so not because of actual geothermal heating, but because the Na-K-Ca, Na/K, and silica geothermometers fail to properly describe equilibrium conditions in low-temperature waters. Thus, it seems unlikely that the hot springs or any other analyzed waters in the southern Cascades of Washington are related to a high temperature geothermal heat source.

The results of the heat flow study leave little doubt that the gravity anomaly associated with the Indian Heaven fissure zone is not caused by a large, still-molten magma chamber. The most likely causes of the gravity anomaly are two: a greater thickness of low density rocks under the fissure zone than was anticipated and the use of an incorrect Bouguer reduction density such that part of the anomaly is caused by the topography itself (compare the gravity contours in fig. 3 with the topographic contours). The average density for all the sedimentary rocks sampled (see table 5) is $2.01 \text{ gm}/\text{cm}^3$. The differential relief of the fissure zone with respect to its surroundings is 300 m to 600 m or more. A horizontal infinitely extended slab 300 m thick with a density contrast of $0.7 \text{ gm}/\text{cm}^3$ would cause an anomaly of about 10 mgal. Therefore, much of the residual anomaly could be caused by topography alone. Furthermore, if there is a thickening of the sedimentary units in the fissure zone area (Hammond and others, 1976), then the density contrast between the sediments and a dense volcanic basement could cause the remainder of the residual gravity anomaly.

It was anticipated that great difficulty would be encountered in obtaining good heat-flow values in the Cascade Range, particularly in holes as shallow as 150 m; however, it is clear that every hole that went to a depth of 150 m gives a reliable heat-flow value and at least 3 of the 4 deep holes would also

yield reasonably accurate (± 15 percent) heat-flow values at depths of 50 m to 100 m and above if corrections were made for various surface conditions. Therefore, these data prove that heat flow studies can be valuable in an area of high rainfall. These holes also furnish the most reliable regional heat-flow data available for the Cascades. These data can be used as background information for continued geothermal studies at other sites in the Cascades.

CONCLUSIONS

1. Heat flow can be successfully measured in relatively shallow holes in areas of high precipitation like Washington's southern Cascade Range.
2. Heat-flow values measured in the Indian Heaven area appear to be of the magnitude expected of typical regional heat-flow values for the Cascade Range.
3. There is no major, shallow heat-flow anomaly (geothermal heat source) in the Indian Heaven area.
4. Temperature gradients in the Indian Heaven area are somewhat higher than normal, leaving open the possibility that waters from depths of 2 km, at about 100°C, or 4 km, at about 200°C, might be usable for industrial or agricultural uses, or even electrical generation. However, the cost of drilling wells to those depths, the lack of knowledge about the availability of ground water at those depths, and the lack of energy-consuming population centers or industry in the immediate area probably rule out any attempts to develop geothermal resources in the Indian Heaven area, at least for the near future.
5. The heat-flow values measured in the Indian Heaven area cannot be used to determine the geothermal potential of either Mount Adams or Mount St. Helens.
6. Water flow through some of the Quaternary basalts (DGER 6) and difficult drilling conditions in those basalts indicate the need for caution in drilling heat-flow holes in the Quaternary basalts.
7. Geochemically estimated source temperatures (Na-K-Ca method) for thermal spring waters in Skamania County are below 100°C. It appears that these waters could have been heated to their estimated temperatures of last equilibration simply by circulating to a depth of one kilometer, more or less, under the influence of a geothermal gradient of 50°C/km.
8. Almost the only geochemically estimated source temperatures (Na-K-Ca method) above 100°C anywhere in Washington's Cascade Range are for thermal or mineral springs within 30 km of Mount Baker, Glacier Peak, or Mount Rainier. This cannot be taken to mean that no other area in the Cascades has geothermal potential, but it is a positive indication that at least three of Washington's five large stratovolcanoes do have some geothermal potential. The absence of thermal or mineral springs around Mount St. Helens or Mount Adams is puzzling, but can perhaps be explained. Yuhara (1974) has found that hot springs are much more likely to be found associated with a stratovolcano whose volcanic edifice has been breached by erosion than with a stratovolcano whose cone is still well-preserved. Mount St. Helens and Mount Adams are certainly better preserved than Mount Baker, Glacier Peak, or

44 HEAT FLOW STUDIES

Mount Rainier, so perhaps their geothermal systems are still well hidden within a ground-water system that is buried under an extensive cover of porous volcanic rock.

9. The gravity anomaly associated with the Indian Heaven area is probably caused by a thicker than anticipated Tertiary sedimentary rock section beneath the northern end of the fissure zone and by the use of a Bouguer reduction density that is too high.
 10. The measurement of bottom-hole temperatures during drilling of the heat-flow holes was successful in providing temperatures that could have been used to estimate equilibrium gradients if the drill holes had been lost because of caving, mechanical problems, or intrabore water circulation.
 11. Additional geophysical studies should be done in the Cascades of Washington in order to more accurately define the heat-flow pattern, and to determine whether heated bodies of ground water and(or) rock exist at depth in the crust, particularly around the major strato-volcanoes.
 12. It appears that the basalts of the Indian Heaven area were erupted from narrow dikes that cooled fairly rapidly at the close of each eruptive phase. If magma chambers formed, they are small and cool, or if still hot they are located away from our heat-flow holes and were not detected.
-

APPENDIX
EQUILIBRIUM TEMPERATURE-DEPTH MEASUREMENTS

Drill hole: DGER-2
Date measured: 9/13/76

Depth (m)	Depth (ft)	Temperature		Geothermal gradient	
		°C	°F	°C/km	°F/100 ft
10.0	32.8	6.110	43.00	.0	.0
15.0	49.2	6.180	43.12	14.0	.8
20.0	65.6	6.240	43.23	12.0	.7
25.0	82.0	6.290	43.32	10.0	.5
30.0	98.4	6.310	43.36	4.0	.2
35.0	114.8	6.350	43.43	8.0	.4
40.0	131.2	6.380	43.48	6.0	.3
45.0	147.6	6.390	43.50	2.0	.1
50.0	164.0	6.840	44.31	90.0	4.9
55.0	180.4	6.820	44.28	-4.0	-.2
60.0	196.8	6.740	44.13	-16.0	-.9
65.0	213.2	6.780	44.20	8.0	.4
70.0	229.6	6.860	44.35	16.0	.9
75.0	246.0	6.820	44.28	-8.0	-.4
80.0	262.4	7.270	45.09	90.0	4.9
85.0	278.8	8.210	46.78	188.0	10.3
90.0	295.2	8.880	47.98	134.0	7.4
95.0	311.6	9.190	48.54	62.0	3.4
100.0	328.0	9.500	49.10	62.0	3.4
105.0	344.4	9.720	49.50	44.0	2.4
110.0	360.8	10.060	50.11	68.0	3.7
115.0	377.2	10.360	50.65	60.0	3.3
120.0	393.6	10.620	51.12	52.0	2.9
125.0	410.0	10.880	51.58	52.0	2.9
130.0	426.4	11.180	52.12	60.0	3.3
135.0	442.8	11.410	52.54	46.0	2.5
140.0	459.2	11.650	52.97	48.0	2.6
145.0	475.6	11.910	53.44	52.0	2.9
150.0	492.0	12.190	53.94	56.0	3.1

Drill hole: DGER-2
Date measured: 10/8/75

Depth (m)	Depth (ft)	Temperature		Geothermal gradient	
		°C	°F	°C/km	°F/100 ft
5.0	16.4	7.050	44.69	.0	.0
10.0	32.8	6.490	43.68	-112.0	-6.1
15.0	49.2	6.720	44.10	46.0	2.5
20.0	65.6	6.500	43.70	-44.0	-2.4
25.0	82.0	6.410	43.54	-18.0	-1.0

Continued

Drill hole: DGER-2—Continued
Date measured: 10-8-75

Depth (m)	Depth (ft)	Temperature		Geothermal gradient	
		°C	°F	°C/km	°F/100 ft
30.0	98.4	6.420	43.56	2.0	.1
35.0	114.8	6.420	43.56	.0	.0
40.0	131.2	6.440	43.59	4.0	.2
45.0	147.6	6.440	43.59	.0	.0
50.0	164.0	6.610	43.90	34.0	1.9
55.0	180.4	6.650	43.97	8.0	.4
60.0	196.8	6.585	43.85	-18.0	-.7
65.0	213.2	6.620	43.92	7.0	.4
70.0	229.6	6.710	44.08	18.0	1.0
75.0	246.0	6.740	44.13	6.0	.3
80.0	262.4	7.100	44.78	72.0	4.0
85.0	278.8	7.990	46.38	178.0	9.8
90.0	295.2	8.100	46.38	22.0	1.2
95.0	311.6	8.650	47.57	110.0	6.0
100.0	328.0	9.090	48.36	88.0	4.8
105.0	344.4	9.500	49.10	82.0	4.5
110.0	360.8	10.110	50.20	122.0	6.7
115.0	377.2	10.400	50.72	88.0	3.2
120.0	393.6	10.680	51.22	86.0	3.1
125.0	410.0	10.840	51.51	32.0	1.8
130.0	426.4	11.170	52.11	66.0	3.6
135.0	442.8	11.420	52.56	30.0	2.7
140.0	459.2	11.675	53.01	31.0	2.8
145.0	475.6	11.910	53.44	47.0	2.6
150.0	492.0	12.180	53.92	54.0	3.0
153.1	502.2	12.340	54.21	51.6	2.8

Drill hole: DGER-3
Date measured: 9/13/76

Depth (m)	Depth (ft)	Temperature		Geothermal gradient	
		°C	°F	°C/km	°F/100 ft
10.0	32.8	5.210	41.38	.0	.0
15.0	49.2	5.900	42.62	138.0	7.6
20.0	65.6	6.060	42.91	32.0	1.8
25.0	82.0	6.330	43.39	54.0	3.0
30.0	98.4	6.630	43.93	60.0	3.3
35.0	114.8	6.860	44.35	46.0	2.5
40.0	131.2	7.160	44.89	60.0	3.3
45.0	147.6	7.490	45.48	66.0	3.6
50.0	164.0	7.810	46.06	64.0	3.5
55.0	180.4	8.110	46.60	60.0	3.3
60.0	196.8	8.490	47.28	76.0	4.2
65.0	213.2	8.730	47.71	48.0	2.6
70.0	229.6	9.050	48.29	64.0	3.5

Continued

Drill hole: DGER-3—Continued
Date measured: 9/13/76

Depth (m)	Depth (ft)	Temperature		Geothermal gradient	
		°C	°F	°C/km	°F/100 ft
75.0	246.0	9.290	48.72	48.0	2.6
80.0	262.4	9.480	49.06	38.0	2.1
85.0	278.8	9.600	49.28	24.0	1.3
90.0	295.2	9.920	49.86	64.0	3.5
95.0	311.6	10.210	50.38	58.0	3.2
100.0	328.0	10.280	50.50	14.0	.8
105.0	344.4	10.580	51.04	60.0	3.3
110.0	360.8	10.730	51.31	30.0	1.6
115.0	377.2	10.880	51.58	30.0	1.6
120.0	393.6	11.350	52.43	94.0	5.2
125.0	410.0	11.460	52.63	22.0	1.2
130.0	426.4	11.760	53.17	60.0	3.3
135.0	442.8	12.110	53.80	70.0	3.8
140.0	459.2	12.400	54.32	58.0	3.2
145.0	475.6	12.690	54.84	58.0	3.2
150.0	492.0	12.980	55.36	58.0	3.2

Drill hole: DGER-3
Date measured: 10/8/75

Depth (m)	Depth (ft)	Temperature		Geothermal gradient	
		°C	°F	°C/km	°F/100 ft
5.0	16.4	6.390	43.50	.0	.0
10.0	32.8	5.740	42.33	-130.0	-7.1
15.0	49.2	6.350	43.43	122.0	6.7
20.0	65.6	6.490	43.68	28.0	1.5
25.0	82.0	6.640	43.95	30.0	1.6
30.0	98.4	6.780	44.20	28.0	1.5
35.0	114.8	6.970	44.55	38.0	2.1
40.0	131.2	7.250	45.05	56.0	3.1
45.0	147.6	7.560	45.61	62.0	3.4
50.0	164.0	7.880	46.18	64.0	3.5
55.0	180.4	8.180	46.72	60.0	3.3
60.0	196.8	8.510	47.32	66.0	3.6
65.0	213.2	8.700	47.66	38.0	2.1
70.0	229.6	8.940	48.09	48.0	2.6
75.0	246.0	9.280	48.70	68.0	3.7
80.0	262.4	9.520	49.14	48.0	2.6
85.0	278.8	9.620	49.32	20.0	1.1
90.0	295.2	9.950	49.91	66.0	3.6
95.0	311.6	10.200	50.36	50.0	2.7
100.0	328.0	10.350	50.63	30.0	1.6
105.0	344.4	10.610	51.10	52.0	2.9
110.0	360.8	10.680	51.22	14.0	.8
115.0	377.2	10.900	51.62	44.0	2.4

Continued

Drill hole: DGER-3—Continued
Date measured: 10/8/75

Depth (m)	Depth (ft)	Temperature		Geothermal gradient	
		°C	°F	°C/km	°F/100 ft
120.0	393.6	11.270	52.29	74.0	4.1
125.0	410.0	11.540	52.77	64.0	3.0
130.0	426.4	11.820	53.28	56.0	3.1
135.0	442.8	12.100	53.78	56.0	3.1
140.0	459.2	12.390	54.30	58.0	3.2
145.0	475.6	12.680	54.82	58.0	3.2
150.0	492.0	12.970	55.35	58.0	3.2
152.5	500.2	13.120	55.62	60.0	3.3

Drill hole: DGER-4
Date measured: 9/14/76

Depth (m)	Depth (ft)	Temperature		Geothermal gradient	
		°C	°F	°C/km	°F/100 ft
5.0	16.4	3.270	37.89	.0	.0
10.0	32.8	3.270	37.89	.0	.0
15.0	49.2	3.560	38.41	58.0	3.2
20.0	65.6	3.720	38.70	32.0	1.8
25.0	82.0	3.870	38.97	30.0	1.6
30.0	98.4	4.000	39.20	26.0	1.4
35.0	114.8	4.130	39.43	26.0	1.4
40.0	131.2	4.260	39.67	26.0	1.4
45.0	147.6	4.390	39.90	26.0	1.4
50.0	164.0	4.520	40.14	26.0	1.4
55.0	180.4	4.680	40.42	32.0	1.8
60.0	196.8	4.820	40.68	28.0	1.5
65.0	213.2	4.990	40.98	34.0	1.9
70.0	229.6	5.160	41.29	34.0	1.9
75.0	246.0	5.320	41.58	32.0	1.8
80.0	262.4	5.600	42.08	56.0	3.1
85.0	278.8	5.780	42.40	36.0	2.0
90.0	295.2	6.060	42.91	56.0	3.1
95.0	311.6	6.300	43.34	48.0	2.6
100.0	328.0	6.550	43.79	50.0	2.7
105.0	344.4	6.780	44.20	46.0	2.5
110.0	360.8	6.980	44.56	40.0	2.2
115.0	377.2	7.200	44.96	44.0	2.4
120.0	393.6	7.460	45.43	52.0	2.9
125.0	410.0	7.710	45.88	50.0	2.7
130.0	426.4	7.970	46.35	52.0	2.9
135.0	442.8	8.200	46.76	46.0	2.5
140.0	459.2	8.460	47.23	52.0	2.9
145.0	475.6	8.720	47.70	52.0	2.9
150.0	492.0	8.950	48.11	46.0	2.5
152.5	500.2	9.100	48.38	60.0	3.3

Drill hole: DGER-4
Date measured: 10/8/75

Depth (m)	Depth (ft)	Temperature		Geothermal gradient	
		°C	°F	°C/km	°F/100 ft
5.0	16.4	4.620	40.32	.0	.0
10.0	32.8	3.720	38.70	-180.0	-9.9
15.0	49.2	3.900	39.02	36.0	2.0
20.0	65.6	4.030	39.25	26.0	1.4
25.0	82.0	4.160	39.49	26.0	1.4
30.0	98.4	4.250	39.65	18.0	1.0
35.0	114.8	4.370	39.87	24.0	1.3
40.0	131.2	4.490	40.08	24.0	1.3
45.0	147.6	4.620	40.32	26.0	1.4
50.0	164.0	4.750	40.55	26.0	1.4
55.0	180.4	5.000	41.00	50.0	2.7
60.0	196.8	5.750	42.35	150.0	8.2
65.0	213.2	5.870	42.57	24.0	1.3
70.0	229.6	5.950	42.71	16.0	.9
75.0	246.0	5.630	42.13	-64.0	-3.5
80.0	262.4	5.740	42.33	22.0	1.2
85.0	278.8	5.850	42.53	22.0	1.2
90.0	295.2	6.085	42.95	47.0	2.6
95.0	311.6	6.330	43.39	49.0	2.7
100.0	328.0	6.550	43.79	44.0	2.4
105.0	344.4	6.780	44.20	46.0	2.5
110.0	360.8	6.970	44.55	38.0	2.1
115.0	377.2	7.220	45.00	50.0	2.7
120.0	393.6	7.470	45.45	50.0	2.7
125.0	410.0	7.720	45.90	60.0	2.7
130.0	426.4	7.960	46.33	48.0	2.6
135.0	442.8	8.210	46.78	50.0	2.7
140.0	459.2	8.460	47.23	50.0	2.7
145.0	475.6	8.710	47.68	50.0	2.7
150.0	492.0	8.960	48.13	50.0	2.7
152.7	500.9	9.110	48.40	55.6	3.0

Drill hole: DGER-5
Date measured: 9/14/76

Depth (m)	Depth (ft)	Temperature		Geothermal gradient	
		°C	°F	°C/km	°F/100 ft
10.0	32.8	5.930	42.67	.0	.0
15.0	49.2	6.110	43.00	36.0	2.0
20.0	65.6	6.180	43.12	14.0	.8
25.0	82.0	6.240	43.23	12.0	.7
30.0	98.4	6.330	43.39	18.0	1.0
35.0	114.8	6.440	43.59	22.0	1.2
40.0	131.2	6.550	43.79	22.0	1.2
45.0	147.6	6.710	44.08	32.0	1.8
50.0	164.0	6.900	44.42	38.0	2.1

Continued

Drill hole: DGER-5—Continued
Date measured: 9/14/76

Depth (m)	Depth (ft)	Temperature		Geothermal gradient	
		°C	°F	°C/km	°F/100 ft
55.0	180.4	7.070	44.73	34.0	1.9
60.0	196.8	7.300	45.14	46.0	2.5
65.0	213.2	7.440	45.39	28.0	1.5
70.0	229.6	7.670	45.81	46.0	2.5
75.0	246.0	7.900	46.22	46.0	2.5
80.0	262.4	8.160	46.69	52.0	2.9
85.0	278.8	8.350	47.03	38.0	2.1
90.0	295.2	8.530	47.35	36.0	2.0
95.0	311.6	8.710	47.68	36.0	2.0
100.0	328.0	8.910	48.04	40.0	2.2
105.0	344.4	9.170	48.51	52.0	2.9
110.0	360.8	9.450	49.01	56.0	3.1

Total depth of 150 m not reached because of blockage.
See temperature-depth log of 10/9/75.

Drill hole: DGER-5
Date measured: 10/9/75

Depth (m)	Depth (ft)	Temperature		Geothermal gradient	
		°C	°F	°C/km	°F/100 ft
5.0	16.4	6.970	44.55	.0	.0
10.0	32.8	6.230	43.21	-148.0	-8.1
15.0	49.2	6.230	43.21	.0	.0
20.0	65.6	6.290	43.32	12.0	.7
25.0	82.0	6.340	43.41	10.0	.5
30.0	98.4	6.420	43.56	16.0	.9
35.0	114.8	6.520	43.74	20.0	1.1
40.0	131.2	6.620	43.92	20.0	1.1
45.0	147.6	6.750	44.15	26.0	1.4
50.0	164.0	6.930	44.47	36.0	2.0
55.0	180.4	7.110	44.80	36.0	2.0
60.0	196.8	7.290	45.12	36.0	2.0
65.0	213.2	7.480	45.46	38.0	2.1
70.0	229.6	7.690	45.84	42.0	2.3
75.0	246.0	7.940	46.29	50.0	2.7
80.0	262.4	8.250	46.85	62.0	3.4
85.0	278.8	8.370	47.07	24.0	1.3
90.0	295.2	8.550	47.39	36.0	2.0
95.0	311.6	8.740	47.73	38.0	2.1
100.0	328.0	8.960	48.13	44.0	2.4
105.0	344.4	9.200	48.56	48.0	2.6
110.0	360.8	9.460	49.03	52.0	2.9
115.0	377.2	9.780	49.60	64.0	3.5
120.0	393.6	9.960	49.93	36.0	.0

Continued

Drill hole: DGER-5—Continued
Date measured: 10/9/75

Depth (m)	Depth (ft)	Temperature		Geothermal gradient	
		°C	°F	°C/km	°F/100 ft
125.0	410.0	10.230	50.41	54.0	.0
130.0	426.4	10.500	50.90	54.0	3.0
135.0	442.8	10.750	51.35	50.0	2.7
140.0	459.2	11.010	51.82	62.0	2.9
145.0	475.6	11.250	52.25	48.0	2.6
150.0	492.0	11.500	52.70	50.0	2.7

Drill hole: DGER-6
Date measured: 9/14/76

Depth (m)	Depth (ft)	Temperature		Geothermal gradient	
		°C	°F	°C/km	°F/100 ft
5.0	16.4	2.600	36.68	.0	.0
10.0	32.8	2.610	36.70	2.0	.1
15.0	49.2	2.630	36.73	4.0	.2
20.0	65.6	2.620	36.72	-2.0	-.1
25.0	82.0	2.640	36.75	4.0	.2
30.0	98.4	2.690	36.84	10.0	.5
35.0	114.8	2.720	36.90	6.0	.3
40.0	131.2	2.740	36.93	4.0	.2
45.0	147.6	2.750	36.95	2.0	.1
50.0	164.0	2.730	36.91	-4.0	-.2
55.0	180.4	2.710	36.88	-4.0	-.2

Drill hole: DGER-6
Date measured: 10/8/75

Depth (m)	Depth (ft)	Temperature		Geothermal gradient	
		°C	°F	°C/km	°F/100 ft
5.0	16.4	3.320	37.98	.0	.0
10.0	32.8	2.680	36.82	-128.0	-7.0
15.0	49.2	3.050	37.49	74.0	4.1
20.0	65.6	3.030	37.45	-4.0	-.2
25.0	82.0	2.980	37.36	-10.0	-.5
30.0	98.4	3.020	37.44	8.0	.4
35.0	114.8	2.940	37.29	-16.0	-.9
40.0	131.2	3.200	37.76	62.0	2.9
45.0	147.6	3.210	37.78	2.0	.1
50.0	164.0	3.050	37.49	-32.0	-1.8
55.0	180.4	2.940	37.29	-22.0	-1.2
55.7	182.7	2.930	37.27	-14.3	-.8

Drill hole: DGER-7
Date measured: 9/14/76

Depth (m)	Depth (ft)	Temperature		Geothermal gradient	
		°C	°F	°C/km	°F/100 ft
10.0	32.8	2.840	37.11	.0	.0
15.0	49.2	2.850	37.13	2.0	.1
20.0	65.6	3.240	37.83	78.0	4.3
25.0	82.0	3.550	38.39	62.0	3.4

Drill hole: DGER-7
Date measured: 10/8/75

Depth (m)	Depth (ft)	Temperature		Geothermal gradient	
		°C	°F	°C/km	°F/100 ft
5.0	16.4	6.580	43.84	.0	.0
10.0	32.8	5.160	41.29	-234.0	-15.6
15.0	49.2	3.080	37.54	-416.0	-22.8
20.0	65.6	3.360	38.05	56.0	3.1
25.0	82.0	3.630	38.53	54.0	3.0
28.6	93.8	3.810	38.86	60.0	2.7

REFERENCES CITED

- Allen, J. E. 1966, The Cascade Range volcano-tectonic depression of Oregon. In Transactions of the Lunar Geological Field Conference, Bend, Oregon: Oregon Department of Geology and Mineral Industries, p. 21-23.
- Atwater, Tanya, 1970, Implications of plate tectonics for the Cenozoic tectonic evolution of western North America: Geological Society of America Bulletin, v. 81, No. 12, p. 3513-3535.
- Birch, A. F., 1950, Flow of heat in the Front Range, Colorado: Geological Society of America Bulletin, v. 61, No. 6, p. 567-630.
- Blackwell, D. D., 1971, The thermal structure of the continental crust. In Heacock, John G., editor. The structure and physical properties of the earth's crust: American Geophysical Union Geophysical Monograph 14, p. 169-184.
- Blackwell, D. D., 1974, Terrestrial heat flow and its implications on the location of geothermal reservoirs in Washington. In Energy Resources of Washington: Washington Division of Geology and Earth Resources Information Circular 50, p. 21-33.
- Blackwell, D. D.; and others, 1973, Heat flow and Cenozoic tectonic history of the northwestern United States [abstract]: Geological Society of America Abstracts with Programs, v. 5, No. 1, p. 12-13.
- Blackwell, D. D.; Baag, Czang-Go, 1973, Heat flow in a "blind" geothermal area near Marysville, Montana: Geophysics, v. 38, No. 5, p. 941-956.
- Bonini, W. E.; Hughes, D. W.; Daneš, Z. F., 1974, Complete Bouguer gravity anomaly map of Washington: Washington Division of Geology and Earth Resources Geologic Map GM-11.
- Campbell, K. V.; and others, 1970, A survey of thermal springs in Washington State: Northwest Science, v. 44, No. 1, p. 1-11.
- Combs, Jim; Muffler, L. J. P., 1973, Exploration for geothermal resources. In Kruger, Paul; Otte, Carel, editors, Geothermal energy; resources, production, stimulation: Stanford University Press, Stanford, California, p. 95-128.
- Crandell, D. R.; Miller, R. D., 1974, Quaternary stratigraphy and extent of glaciation in the Mount Rainier region, Washington: U.S. Geological Society Professional Paper 847, 59 p.
- Crandell, D. R.; Mullineaux, D. R., 1973, Pine Creek volcanic assemblage at Mount St. Helens, Washington: U.S. Geological Survey Bulletin 1383-A, 23 p.
- Crosson, R. S., 1972, Small earthquakes, structure, and tectonics of the Puget Sound region: Seismological Society of America Bulletin, v. 62, No. 5, p. 1133-1171.
- Crosson, R. S., 1974, Compilation of earthquake hypocenters in western Washington: Washington Division of Geology and Earth Resources Information Circular 53, 25 p.
- Fischer, J. F., 1971, The geology of the White River-Carbon Ridge area, Cedar Lake quadrangle, Cascade Mountains, Washington: University of California at Santa Barbara Ph.D. thesis, 200 p.
- Fiske, R. S.; Hopson, C. A.; Waters, A. C., 1963, Geology of Mount Rainier National Park, Washington: U.S. Geological Survey Professional Paper 444, 93 p.

54 REFERENCES CITED

- Fournier, R. O.; Truesdell, A. H., 1970, Chemical indicators of subsurface temperature applied to hot spring waters of Yellowstone National Park, Wyoming, U.S.A. In Proceedings of the United Nations Symposium on the Development and Utilization of Geothermal Resources, Pisa, Italy, 22 September-1 October, 1970: Geothermics, Special Issue 2, v. 2, part 1, p. 529-535.
- Fournier, R. O.; Truesdell, A. H., 1973, An empirical Na-K-Ca geothermometer for natural waters: *Geochemica et Cosmochemica Acta*, v. 37, No. 5, p. 1255-1275.
- Fournier, R. O.; Truesdell, A. H., 1974, Geochemical indicators of subsurface temperature—Part 2, estimation of temperature and fraction of hot water mixed with cold water: *U.S. Geological Survey Journal of Research*, v. 2, No. 3, p. 263-270.
- Gizienski, S. F.; McEuen, R. B.; Birkhahn, P. C., 1975, Regional evaluation of the geothermal resource potential in central Washington State: Washington Public Power Supply System, Richland, Washington, open-file report, 113 p.
- Grant, A. R., 1969, Chemical and physical controls for base metal deposition in the Cascade Range of Washington: Washington Division of Mines and Geology Bulletin 58, 107 p.
- Hammond, P. E., 1973, Preliminary geologic maps of the southern Cascade Range, Washington: Washington Division of Mines and Geology Open-file Report 73-3, 5 sheets.
- Hammond, P. E., 1974, Regional extent of the Stevens Ridge Formation in the southern Cascade Range, Washington [abstract]: *Geological Society of America Abstracts with Programs*, v. 6, No. 3, p. 188.
- Hammond, P. E., 1975, Preliminary geologic map and cross sections with emphasis on Quaternary volcanic rocks, southern Cascade Mountains, Washington: Washington Division of Geology and Earth Resources Open-file Report 75-13, 1 sheet.
- Hammond, P. E.; and others, 1976, Geology and gravimetry of the Quaternary basaltic volcanic field, southern Cascade Range, Washington. In Pezzotti, C., editor. Proceedings of the Second United Nations Symposium on the Development and Use of Geothermal Resources, San Francisco, May 20-29, 1975, v. 1, p. 397-405.
- Harfe, D. S., 1974, Geology of the Babyshoe Ridge area, southern Cascades, Washington: Oregon State University M.S. thesis, 71 p.
- Hartman, D. A., 1973, Geology and low-grade metamorphism of the Greenwater River area, central Cascade Range, Washington: University of Washington Ph.D. thesis, 99 p.
- Holmgren, D. A., 1969, Columbia River Basalt patterns from central Washington to northern Oregon: University of Washington Ph.D. thesis, 56 p.
- Hopkins, K. D., 1969, Late Quaternary glaciation and volcanism on the south slope of Mount Adams, Washington: *Geological Society of America Abstracts with Programs* for 1969, part 3, p. 27.
- Hopkins, K. D., 1976, Geology of the south and east slopes of Mount Adams volcano, Cascade Range, Washington: University of Washington Ph.D. thesis, 143 p.
- Hopson, C. A., 1971, Eruptive sequence at Mount St. Helens, Washington: *Geological Society of America Abstracts with Programs*, v. 3, No. 2, p. 138.

- Kienle, C. F., Jr.; Newcomb, R. C., 1973, Geologic studies of Columbia River Basalt structures and age of deformation, The Dalles-Umatilla region, Washington and Oregon: Shannon and Wilson, Inc., Portland, Oregon, 55 p.
- Konicek, D. L., 1974, Geophysical survey in south-central Washington: University of Puget Sound M.S. thesis, 35 p.
- Konicek, D. L., 1975, Geophysical survey in south-central Washington: Northwest Science, v. 49, No. 2, p. 106-117.
- Lachenbruch, A. H.; Sass, J. H.; Munroe, R. J.; Moses, T. H., Jr., 1976, Geothermal setting and simple heat conduction models for the Long Valley Caldera: Journal of Geophysical Research, v. 81, No. 5, p. 769-784.
- McBirney, A. R.; and others, 1974, Episodic volcanism in the central Oregon Cascade Range: Geology (Geological Society of America), v. 2, No. 12, p. 585-589.
- Mullineaux, D. R., 1974, Pumice and other pyroclastic deposits in Mount Rainier National Park, Washington: U.S. Geological Survey Bulletin 1326, 83 p.
- Mullineaux, D. R.; Hyde, J. H.; Rubin, Meyer, 1975, Widespread late glacial and postglacial tephra deposits from Mount St. Helens volcano, Washington: U.S. Geological Survey Journal of Research, v. 3, No. 3, p. 329-335.
- Newcomb, R. C., 1969, Effect of tectonic structure on the occurrence of ground water in the basalt of the Columbia River Group of The Dalles area, Oregon and Washington: U.S. Geological Survey Professional Paper 383-C, 33 p.
- Pedersen, S. A., 1973, Intraglacial volcanoes of the Crazy Hills area, northern Skamania County, Washington [abstract]: Geological Society of America Abstracts with Programs, v. 5, No. 1, p. 89.
- Renner, J. L.; White, D. E.; Williams, D. L., 1975, Hydrothermal convection system. In White, D. E.; Williams, D. L., editors. Assessment of geothermal resources of the United States—1975: U.S. Geological Survey Circular 726, p. 5-57.
- Roy, R. F.; Blackwell, D. D.; Birch, A. F., 1968, Heat generation of plutonic rocks and continental heat flow provinces: Earth and Planetary Science Letters, v. 5, No. 1, p. 1-12.
- Roy, R. F.; Blackwell, D. D.; Decker, E. R., 1972, Continental heat flow. In Robertson, E. C.; Hays, James F.; Knopoff, Leon, editors. The nature of the solid earth: McGraw-Hill Book Co., New York, p. 506-543.
- Sass, J. H.; and others, 1971, Heat flow in the western United States: Journal of Geophysical Research, v. 76, No. 26, p. 6376-6413.
- Schuster, J. E., 1974, Geothermal energy potential of Washington. In Energy Resources of Washington: Washington Division of Geology and Earth Resources Information Circular 50, p. 1-19.
- Sheppard, R. A., 1964, Geologic map of the Husum quadrangle, Washington: U.S. Geological Survey Mineralogical Investigations Field Studies Map MF-280.
- Sheppard, R. A., 1967, Petrology of a late Quaternary potassium-rich andesite flow from Mount Adams, Washington: U.S. Geological Survey Professional Paper 575-C, p. C55-C59.

56 REFERENCES CITED

- Smith, R. L.; Shaw, H. R., 1975, Igneous-related geothermal systems. In White, D. E.; Williams, D. L., editors. Assessment of geothermal resources of the United States—1975: U.S. Geological Survey Circular 726, p. 58-83.
- Stricklin, C. R., 1975, Geophysical survey of the Lemei Rock-Steamboat Mountain area, Washington: University of Puget Sound M.S. thesis, 23 p.
- Tabor, R. W.; Crowder, D. F., 1969, On batholiths and volcanoes—Intrusion and eruption of late Cenozoic magmas in the Glacier Peak area, North Cascades, Washington: U.S. Geological Survey Professional Paper 604, 67 p.
- Unger, J. D.; Mills, K. F., 1973, Earthquakes near Mount St. Helens, Washington: Geological Society of America Bulletin, v. 84, No. 3, p. 1065-1067.
- United States Geological Survey, 1975, Aeromagnetic map for part of southwestern Washington: U.S. Geological Survey open-file report 75-648, 4 sheets, map scale 1:62,500.
- Van Denburgh, A. S.; Santos, J. F., 1965, Ground water in Washington—Its chemical and physical quality: Washington Division of Water Resources Water Supply Bulletin 24, 93 p.
- Waters, A. C., 1973, The Columbia River Gorge Basalt stratigraphy, ancient lava dams and landslide dams. In Beaulieu, J. D. Geologic field trips in northern Oregon and southern Washington: Oregon Department of Geology and Mineral Industries Bulletin 77, p. 133-162.
- White, D. E., 1970, Geochemistry applied to the discovery, evaluation, and exploitation of geothermal energy resources, rapporteur's report. In Barbier, E. Proceedings of the United Nations Symposium on the Development and Utilization of Geothermal Resources, Pisa, Italy, 1970: Geothermics, Special Issue 2, v. 1, p. 58-80.
- Wise, W. S., 1959, Occurrence of wairakite in metamorphic rocks of the Pacific Northwest: American Mineralogist, v. 44, Nos. 9-10, p. 1099-1101.
- Wise, W. S., 1961, Geology and mineralogy of the Wind River area, Skamania County, Washington, and the stability relations of celadonite: The Johns Hopkins University Ph.D. thesis, 258 p.
- Wise, W. S., 1970, Cenozoic volcanism in the Cascade Mountains of southern Washington: Washington Division of Mines and Geology Bulletin 60, 45 p.
- Yuhara, K., 1974, Morphological, hydrological, and thermal characteristics of active volcanoes having no geothermal areas, and artificial hydrothermal systems for utilizing their latent internal heat energy. In Colp, J. L.; Furumoto, A. S., editors. The utilization of volcano energy: Sandia Laboratory, Albuquerque, New Mexico, p. 391-414.